Doctoral Dissertation

Molecular Mechanisms of Energy Allocation: Identification and Functional Characterization of *DNA Methyltransferase 3.1* in *Daphnia magna* under Starved Conditions

NGUYEN DUC NHAN

March, 2021

International Program of Frontier Biotechnology

Division of Advanced Science and Biotechnology

Graduate School of Engineering

Osaka University

Abstract

Chapter 1 Introduction

Life-history theory predicts that individuals should trade-off energy allocation between reproduction and somatic growth or even survival to maximize lifetime reproductive success. These traits are known to be negatively related to each other, and these antagonistic relationships are called trade-offs. Reproduction fundamentally compromises survival due to trade-offs, and with limited resources, organisms are coped with decisions on whether to invest in maintenance, growth, or reproduction. *Daphnia* has long been a model of energy allocation studies due to its important position in the trophic cascade of freshwater ecosystems. *Daphnia* also allocates energy with various amounts of algae. Under caloric restriction conditions, daphnids use less energy for growth and reproduction and more for maintenance (respiration and carapace formation). Recent whole-genome bisulfite sequencing efforts have revealed that DNA methylation in *Daphnia magna* changes in response to different conditions, including caloric restriction. However, the role of *DNA (cytosine-5) methyltransferases* in *Daphnia magna* for controlling energy allocation between life-history traits in response to caloric restriction remains unknown.

Chapter 2 Cloning and expression analyses of *DNA Methyltransferase* genes in *D. magna*

I first characterized domain structure and expression patterns of *DNMT3* orthologs in *D. magna.* In this species, I identified two DNMT3 orthologs, DapmaDNMT3.1 (DNMT3.1) and DapmaDNMT3.2 (DNMT3.2), which lack the conserved methyltransferase motifs in the catalytic domain and the PWWP domain, respectively. I profiled the expression of the two orthologs during embryogenesis and under various feeding levels. Interestingly, both genes were downregulated in nutrient-rich conditions, whereas *DNMT3.1* was upregulated at the lower food levels, suggesting a potential role of *DNMT3.1* in gene regulation in response to caloric restriction.

Chapter 3 DNMT3.1 controls life span and the trade-off between growth and fecundity under the starved condition

In order to characterize the function of DNMT3.1, I generated a DNMT3.1 mutant by CRISPR/Cas-mediated target mutagenesis. The biallelic mutant was viable and did not show any change in growth rate, reproduction, and longevity under nutrient-rich conditions. However, the

growth rate of this DNMT3.1 mutant was increased. Still, its reproduction was reciprocally reduced compared to the wild type when the growth and reproduction activities competed from instar 4 to 8. We also compared transcriptomes between DNMT3.1 mutant and wild type under nutrient-rich and starved conditions. Consistent with the mutant phenotypes, the starved condition led to changes in the mutant's transcriptomes of the mutant including differential expression of *vitellogenin* genes. In addition, we found upregulation of the *I am not dead yet* (*INDY*) ortholog, which has been known to shorten the life span in *Drosophila*, explaining the shorter life span of the DNMT3.1 mutant. In a previous study, 115 hypermethylated genes were reported under caloric restriction but we found only 8 genes exhibiting differential expression among 2770 DEGs (differentially expressed genes) between wildtype and the mutant line. These results suggested that the DNMT3.1 functions as a regulator for life span and energy allocation between growth and reproduction during caloric restriction.

Chapter 4 General discussion

This study clarified the role of DNMT3.1 in response to caloric restriction. Under starved conditions, I found the upregulation of *DNMT3.1* expression. In addition, I generated DNMT3.1 mutant by CRISPR/Cas-mediated target mutagenesis. During caloric restriction, the mutants showed a trade-off between growth and reproduction by investing more energy to growth and shortening their life span when the growth and reproduction activities competed. Although DNMT3.1 lacks an evolutionarily conserved sequence of the methyltransferase domain, it changes the global transcriptome in response to starvation. In the future, the gene regulatory mechanisms can be investigated not only by investigating DNA methylation but also by chromatin immunoprecipitation for the identification of direct targets of this protein. I anticipate that this work will contribute to understanding the molecular mechanisms underlying energy allocation in the ecologically important *Daphnia* species.

Acknowledgements

Firstly, I would like to express my sincere gratitude to Professor Hajime Watanabe of Department of Biotechnology, Graduate School of Engineer, Osaka University, for his kindness in giving me the great opportunity to do research in Bioenvironmental Science Laboratory and his guidance. Furthermore, I would like to thank Professor Tomoaki Matsuura for his helpful comments and thinking, and special gratitude to Associate Professor Yasuhiko Kato for his personal guidance and teaching in the laboratory.

Secondly, I would like to thank the committee members, Professor Takeshi Omasa and Professor Kohsuke Honda for their thoughtful comments and valuable suggestions on this dissertation.

Next, I would like to acknowledge the Department of Biotechnology, Osaka University and Monbugakusho Scholarship (MEXT) for the financial support.

Thank you to my parents and friends, whose support and encouragements definitely helped and raised me up. Finally, thank you to my incredible soul mate Tien, for making this journey all the more exciting.

Table of Contents

Chapter 1

Introduction

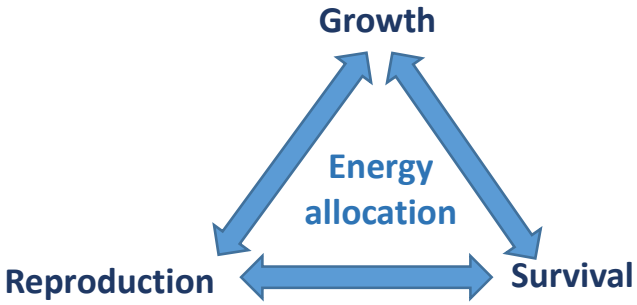

Figure 1.1. Life history theory

Life-history theory predicts that individuals should trade-off energy allocation between reproduction and somatic growth or even survival to maximize lifetime reproductive success [1]. These traits are known to be negatively related to each other, and these antagonistic relationships are called trade-offs (Figure 1.1). Reproduction fundamentally compromises survival due to trade-offs, and with limited resources, organisms are coped with decisions on whether to invest in maintenance, growth, or reproduction.

Due to the finite nature of the energy budget, resource-limited conditions impose changes in resource allocation between competing processes, such as growth, reproduction, and survival. Food limitations change energy allocation to physiologies and affect biological processes, including energy storage, metabolism, oxidative damage, and immune function. Taking lizards as an example, by altering nutrient resources, the physiological costs that influence the trade-off between reproduction and survival could be quantified [2]. This link with physiology has important

consequences for life histories trait and trade-offs. At the physiological level, variation in life-history trade-offs is likely regulated through specific nutrient limitations and how these resources are allocated [3,4]. Pleiotropic physiological mechanisms might regulate resource allocation of energy between traits (such as growth and reproduction) within individuals.

1.1 Caloric restriction and DNA methylation

Caloric restriction or reduction of daily nutrient intake enhances health and life span in animals. The condition increases mitochondrial biogenesis and bioenergetics efficiency leading to regulation of reactive oxygen and maintenance of the mitochondrial ATP production [5]. Therefore, CR is beneficial in resisting various stresses, including heat, oxidation, metabolism, and age-related diseases [6].

DNA methylation, one of the epigenetic regulatory mechanisms, is common in bacteria and eukaryotes. Compared to other regulations such as histone modification, DNA methylation is stable and transmitted to daughter cells after cell division, resulting in gene expression repression. Genomic DNA in mammalian cells commonly undergoes methylation of the cytosine residues at C5 in CpG sequences. DNA methylation of CpG dinucleotides by the transfer of a methyl group from S-adenosyl-L-methionine (AdoMet) at C5 of cytosine is catalyzed by DNA (cytosine-5)-methyltransferases (Dnmts) [7].

Under caloric restriction (CR), methylation of genomic regions tends to be explicitly modified. For instance, in rats, proto-oncogenes' methylation was enhanced, showing their reduction of the expression [8]. The modification of DNA methylation patterns associated with CR can target genomic regions associated with animals' fitness and life extension [8,9].

1.2 DNA (cytosine-5) methyltransferases

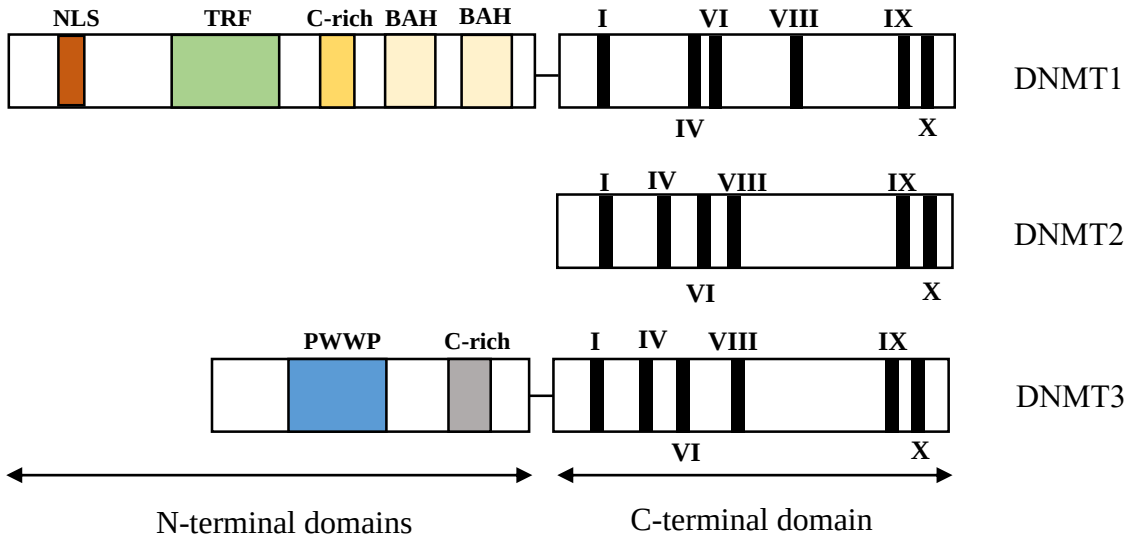

Figure 1.2. Structure of animal DNA methyltransferases. All animal DNA methyltransferases share a highly conserved C-terminal catalytic domain (methyltransferase domain), modified from a previous study [10]. TRF, targeting to replication DNA foci; BAH, Bromo adjacent homology domain; C-rich, cysteine-rich; PWWP, Pro-Trip-Trip-Pro domain; NLS, nuclear localization signal. Roman numerals indicate the major conservative motifs of the C-terminal catalytic domain.

Based on their amino acid sequences, these proteins can be subdivided into three groups that may have distinct functional specificities (Fig.1.2). Dnmt1 and Dnmt3 proteins are defined by their distinct N-terminal domains that mediate various protein-protein interactions. Dnmt2 methyltransferases are defined by their lack of an N-terminal domain and consist of a methyltransferase domain only. Dnmt1 functions as a maintenance methyltransferase that copies methylation patterns from the methylated parental strand to the newly synthesized daughter strand. This activity distinguishes Dnmt1 enzymes from the Dnmt3 *de novo* methyltransferases, which prefer unmethylated DNA as substrates and establish DNA methylation patterns during

development. This activity appears to be targeted by interactions with transcription factors and other chromatin-associated proteins. The function of the third subfamily of DNA methyltransferases, the Dnmt2 proteins, remains enigmatic. These enzymes show the highest degree of evolutionary conservation. However, the enzymatic of Dnmt2 is rather low in DNA substrates and much higher on a specific tRNA molecule ($tRNA^{Asp}$).

A great diversity of DNMTs in eukaryotes has been found (Table 1.1) and suggested the existence of different methylation systems.

Table 1.1. Diversity of Eukaryotic DNMTs

Species	Dnmt1	Dnmt2	Dnmt3
Homo sapiens	1	1	3
Mus musculus	1	1	3
Danio rerio	1	1	3
Drosophila melanogaster		1	
Apis mellifera	2	1	1
Nasonia vitripennis	3	1	1
Daphnia magna	1	1	2

In mammals, methylation occurs predominantly at the symmetrical dinucleotide CpG and defines a tissue-specific pattern concerning 60%-90% of the CpGs throughout the genome [11]. This methylation pattern is set up in the early embryo by the *de novo* MTases DNMT3a/b and is mostly maintained during the development by the maintenance activity of DNMT1 [12]. Numerous studies have revealed a strong negative correlation between DNA methylation of the promoter region and

gene expression [13], and these Mtases are indispensable for normal development [13]. DNMT1 is ubiquitously and highly expressed in proliferating cells, representing the major DNA Mtase activity in somatic tissues throughout mammalian development and is present only at low levels in non-dividing cells. Cell cycle-dependent transcription factors activate *Dnmt1* expression in the S phase and thus are highly expressed in most mitotic cells [14]. DNMT3a and DNMT3b are highly expressed in embryonic tissues and undifferentiated ES cells and down-regulated in differentiated cells [15]. *Dnmt3a* is maternally provided and predominates in oocytes and early preimplantation embryos. DNMT3A establishes the differential DNA methylation patterns at imprinting control regions (ICR) in male and female gametes[16]. *Dnmt3b* is transcribed upon zygotic gene activation (ZGA) and is robustly expressed by the blastocyst stage, at which time its presence is predominantly restricted to the epiblast lineage [15]. A third *de novo* DNA methyltransferase, DNMT3L, lacks the characteristic N-terminal catalytic domain but is required for DNA methylation, predominantly establishing ICR methylation in gametes [17]. DNMT3L is a crucial activating cofactor of DNMT3A/B, explaining its methylation effects despite the lack of inherent catalytic activity [18].

In insects, fruit fly, *DNMT1* and *DNMT3* genes do not exist. However, it has a sparingly methylated genome without a clearly defined functional significance of methylated sites. On the other hand, discovering a functional methylation system in the honeybee, consisting of two *Dnmt1* genes and one copy each of *Dnmt2* and *Dnmt3,* provided the first indication for the existence of both *de novo* and maintenance methylation in insects [19]. Subsequently, an increasing number of insect genomes have been sequenced, showing a large diversity in the number of *Dnmt* genes present [20]. Methylation in adult honeybees (*Apis mellifera)* seems to be restricted to CpG dinucleotides. It occurs mainly in gene bodies, particularly in the proximity of alternatively spliced

exons, suggesting a role in splicing regulation [19]. In 2008, Kucharski showed that siRNA-mediated silencing of the expression of *Dnmt3* in newly hatched honeybee larvae gave rise to the development of adult worker bees with developed ovaries, which is normally associated with queen development only [21]. Further roles for *Dnmt3* in the honeybee have been shown in the regulation of behavior and long-term memory [21,22]. In addition, the observation of lethality associated with *Dnmt3* silencing in embryos suggests a crucial role during embryonic development [23]. Conclusively, *de novo* DNA methylation is essential for honey bee's developmental processes, and it may suggest this feature would be general throughout the insects.

1.3 Model organism: *Daphnia magna*

Daphnia magna

The cladoceran crustacean *Daphnia magna* has long been used for studies of energy allocation for many reasons. Remarkably, *Daphnia magna* occupies an important position in the trophic network of freshwater ecosystems, linking producers and secondary consumers. It can be easily propagated as a cloned individual with a short life cycle by parthenogenetic reproduction. In addition, it can be easily manipulated both in a field and laboratory. Energy allocation of *Daphnia* fed with various amounts of algae has been investigated in order to develop a model of the interaction between the algae and *D. magna* populations [24–27].

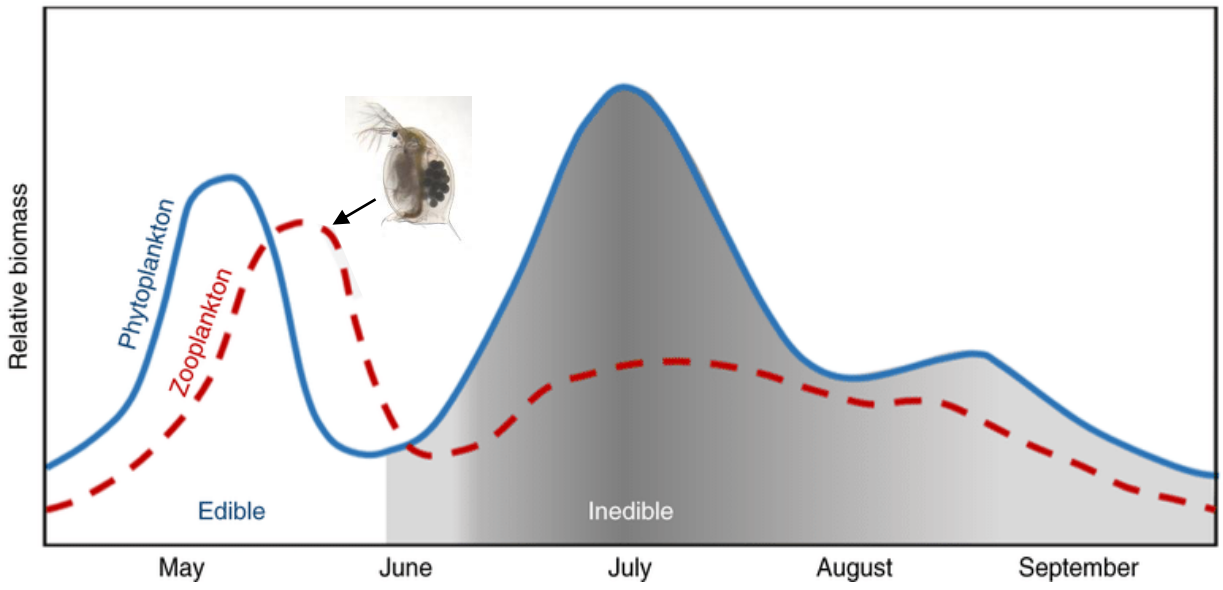

Figure 1.3. Seasonal biomass patterns in phytoplankton and zooplankton. Blue solid line indicates biomass pattern of phytoplankton, including edible and inedible (shading background) for zooplankton. The red dash line indicates the biomass pattern of zooplankton. The figure was modified from a previous review of the plankton ecology group (PEG) model [28].

Based on the relative biomass of zooplankton and phytoplankton, that is depicted on a model at the given time (figure 1.3). It shows that *Daphnia sp. (zooplankton)* annually copes with starvation due to the edible algae season. Following a previous study, under caloric restriction conditions, daphnids use less energy for growth and reproduction and more for maintenance (respiration and carapace formation) [27].

Recently, the *D. magna* genome has been sequenced [29,30], and CRISPR/Cas-based genome editing technology has been established to introduce indel mutations at the targeted locus [31,32]. However, these genetic tools have not yet been used to analyze genes involved in energy allocation.

1.4 Aim of this study

In many instances, the trade-offs of life-history traits might involve physiological, behavioral, morphological, or ecological factors and response at the genomic level (for example, changes in transcription rates). Therefore, genomics can figure out the question of how a trade-off that is expressed at the phenotypic level is manifested or modulated at the level of genetic regulation. In *Drosophila melanogaster,* genes affecting life-history traits have been investigated in controlling lifespan and fecundity, such as *Forkhead box O* (Foxo) [35], and *I am not dead yet (Indy)* [36]. In this study, I aim to investigate what gene controls energy allocation between life-history traits in *Daphnia magna.*

The following two chapters are comprised of all experimental summaries, which are helping me to clarify the question. Chapter Two describes the first evidence that a well-characterized *DNMT3* gene in *Daphnia magna.* I examined two DNMT3 orthologs in *Daphnia magna*, DapmaDNMT3.1 (DNMT3.1) and DapmaDNMT3.2 (DNMT3.2). Amino acid sequence alignment revealed that DNMT3.1 and DNMT3.2 lack the conserved methyltransferase motifs of the catalytic domain and the PWWP domain, respectively. Then, I profiled the expression of the two orthologs during embryogenesis and under various feeding levels. Chapter Three follows up on this work by generating CRISPR/Cas-mediated target mutagenesis of DNA methyltransferase 3.1 (DNMT3.1) that is upregulated in response to caloric restriction in *Daphnia magna.* After establishing the mutant line, I observed life-history trait changes of the mutants compared to wild types under nutrient-rich and starved conditions. Finally, I also compared transcriptomes between DNMT3.1 mutant and wild type under the two conditions.

Chapter 2

Cloning and expression analyses of *DNA Methyltransferase* genes in *Daphnia magna*

2.1 Introduction

DNA methylation is a major, heritable epigenetic modification involved in gene regulation commonly observed in eukaryotes [13]. It plays essential roles in various biological events, including development [37], phenotypic plasticity, and disease [38]. In animals, cytosine DNA methylation is predominantly found at CpG dinucleotides, which is an essential epigenetic mark in gene-regulatory systems, including transcriptional regulation [39], X-chromosome inactivation [40], and genomic imprinting [41]. Besides the dynamic genome-wide changes in DNA methylation during development [42], environmental cues lead to *de novo* methylation and shape phenotypic traits and fitness in both vertebrates [43,44] and invertebrates [21,45].

DNA modification is mediated by the DNA (cytosine-5) methyltransferase (DNMT) family, which comprises three classes: DNMT1–3. Mammalian genomes encode six DNMTs: DNMT1, DNMT2, DNMT3A, DNMT3B, DNMT3C, and DNMT3L [46]. DNMT3 functions in *de novo* methylation. It prefers unmethylated DNA as a substrate and establishes new methylation patterns on DNA [13]. The N-terminus of DNMT3A/B consists of two functional domains for chromatin interactions, the ATRX-DNMT3-DNMT3L (ADD) domain and the Pro-Trp-Trp-Pro (PWWP) domain. The PWWP domain is missing in DNMT3L and DNMT3C [12,47,48]. This domain belongs to the Royal domain superfamily, explicitly interacting with the histone H3 tail containing K36me3 [49,50]. The ADD domain is essential for recognizing and interacting with unmethylated histone H3K4 51,52 and DNMT3A/3L complex formation to facilitate *de novo* methylation [18].

Except for DNMT3L, the C-termini of DNMT3 enzymes are essential for the catalytic activity and contain the highly conserved cytosine-5 methyltransferase motifs that are involved in the covalent addition of a methyl group to cytosine [7,53]. Recently released genomes of several insects have revealed a complex and dynamic evolution of the DNMT family in this clade, including expanding DNMT1 in *Apis mellifera* [19] and *Nasonia vitripennis* [19], loss of DNMT3 in *Bombyx mori* [54], and loss of both DNMT1 and DNMT3 in *Drosophila melanogaster* [19]. In contrast to the expansion of DNMT3 in vertebrates, in invertebrates, this protein shows a narrower distribution or is even lost [20].

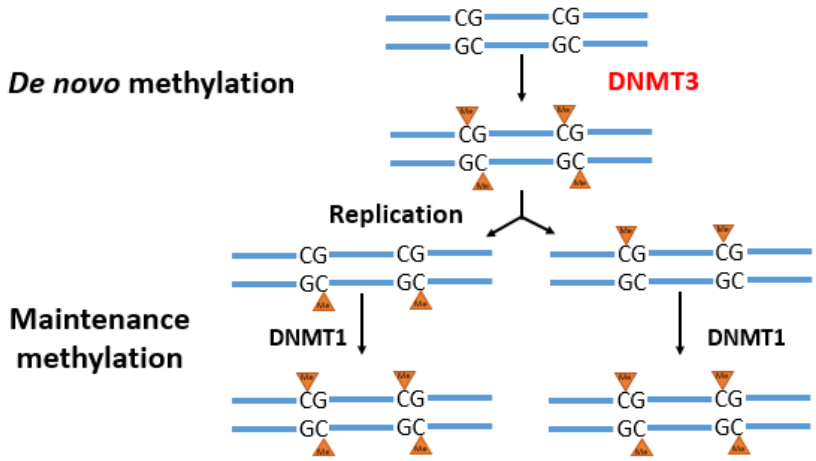

Figure 2.1 Principle of DNMTs mediated *de novo* and maintenance DNA methylation. The solid blue line indicated *De novo* methylation (triangles indicate adding methyl group on cytosines) involves fully unmethylated DNA and is established on both strands (solid blue line). Maintenance of DNA methylation involves hemimethylated DNA.

Daphnia, a freshwater microcrustacean, serves as a model organism in ecological, evolutionary, and environmental sciences. In a healthy environment, daphniids produce genetically identical females by parthenogenesis. These clonal females can change phenotypes in response to various types of environmental stimuli. Under a shortened photoperiod and/or increased population density, reproduction can switch from parthenogenesis to sexual

reproduction [55,56]. Predator cues can induce neck teeth formation [57]. Food quality and caloric restriction affect the growth rate [57] [58]. These features make *Daphnia* an invaluable model for epigenetic study [59]. CpG modifications have been found in two species, *Daphnia magna* and *Daphnia pulex* [60,61]. Recent whole-genome bisulfite sequencing efforts have revealed that DNA methylation in *Daphnia magna* changes in response to salt stress [62], toxic cyanobacteria [63], radioactivity [64], and caloric restriction [65]. The *Daphnia* genome encodes all three enzymes orthologous to mammalian DNMT enzymes [60]. While the above studies suggest the importance of environment-dependent *de novo* DNA methylation in this species, fundamental information on the *de novo* DNMT orthologs, including domain organization, developmental expression, and response to environmental stimuli, is lacking. This study aimed to examine the domain structures of two DNMT3 orthologs, DapmaDNMT3.1, and DapmaDNMT3.2, in *D. magna*. Besides, we profiled their expression during development and under starvation.

2.2 Materials and methods

2.2.1 *D. magna* maintenance

The *D. magna* strain (NIES clone) was obtained from the National Institute for Environmental Studies (NIES; Tsukuba, Japan) and was cultured under laboratory conditions for numerous generations in the Aachener daphnia medium (ADaM) [66]. Briefly, for strain maintenance, 80 individuals were cultured in 5 L of ADaM at 22–24°C, under a 16/8-h light/dark cycle. Daphniids were daily fed 5.6×10^8 *Chlorella* cells/ml during the first week; after maturation, the feeding amount of *Chlorella* was double, and their offspring were removed once per day for maintenance of the population.

2.2.2 Computational identification of DNMT3 ortholog genes in *Daphnia* genomes

A close relationship between crustaceans and insects was clearly shown from the arthropod genomes phylogeny, a valuable source for comparative genomic studies. The bee has a closer relationship with the water flea. The fruit fly was established as a model to analyze the function of DNA methylation systems involving the existence of all three members of DNMT proteins. Therefore, in order to identify DNA methyltransferase genes in *Daphnia*, tblastn searches were performed on the *D. magna* and *D. pulex* genome database via available database from wFleaBase (http://arthropods.eugenes.org/EvidentialGene/daphnia/), using amino acid sequences of DNMT3 in *Apis mellifera* (honeybee) proteins (NP_001177350.1) as queries.

2.2.3 Cloning and sequencing of DapmaDNMT3s

For total RNA extraction, four female adult daphniids were collected and briefly washed. Homogenization was performed with beads using a Micro Smash machine MS-100 (TOMY; Tokyo, Japan) in the presence of Sepasol-RNA I reagent (Nacalai Tesque, Kyoto, Japan) [97]. Total RNA isolation was performed according to the manufacturer's protocol and was followed by phenol/chloroform extractions. One microgram of total RNA was converted to the first-strand cDNA with SuperScript III Reverse Transcriptase (Invitrogen, Carlsbad, CA, USA), using random primers (Invitrogen), according to the manufacturer's protocol. To amplify the ORF of *DapmaDNMT3.1*, primers (*DapmaDNMT3.1*-forward 5'-GTCCAAAATGGCGAATAAAACC-3' and *DapmaDNMT3.1*-reverse 5'-GATTCTGGATTCTCGCATGTCTC-3') were designed to obtain amplicons from a putative start codon to a putative stop codon based on the predicted coding sequence (*Dapma7bEVm006722t1*) in the *D. magna* genome database. Using the cDNA as a template, PCR was performed using KOD-Plus- DNA polymerase (Toyobo, Japan). The amplicon was cloned into a pCR-Blunt II-TOPO vector and sequenced. As the complete ORF of

DapmaDNMT3.2 could not be obtained by PCR-amplified, we decided to amplify part of the ORF. Primers (*DapmaDNMT3.2*-forward 5'- CCCTTGCGTGTTTTGTCTCTC -3' and *DapmaDNMT3.2*-reverse 5'-CGGTAAAATGACGAGGCAGAC-3') were designed based on the predicted coding sequence (*Dapma7bEVm011900t1*). Target DNA fragments were amplified using KOD-Plus-DNA polymerase (Toyobo), cloned into a pCR-Blunt II-TOPO vector, and sequenced.

To obtain the full-length *DapmaDNMT3.2* ORF, 5′ and 3′ rapid amplification of cDNA ends (RACE) was performed using a GeneRacer Kit (Invitrogen) and a SMARTer RACE cDNA Amplification Kit (Clontech Laboratories, Mount View, WI, USA), respectively. The primer sequences used for RACE were as follows:

5′-RACE gene-specific primer (5′-GAACCGGAAAGAGCGAGGCCAAAT-3´)

5′ RACE nested gene-specific primer (5′-GGCCGCAGCAGTCAAAACCTCA-3′)

3′-RACE gene-specific primer (5′-GCCGAGCAAATGACATGGATGG-3′)

In each RACE reaction, target regions were amplified with KOD-Plus-DNA polymerase (Toyobo).

5’ RACE reaction

(Sample reaction)

10x Ex Taq buffer	5 μL
2.5 mM dNTPs mix	4 μL
5 units/μL Ex Taq	0.25 μL
10 μM GeneRacer 5’ primer / 10 μM GeneRacer 5’ nested primer	4.5 μL / 1μL
10 μM st (5’RACE) primer / 10 μM st (5’RACE) nested primer	1.5 μL / 1μL
5’ RACE-ready cDNA / 5’ RACE PCR (nested)	1 μL
miliQ	To 50 μL

(Thermal cycle setting)

	94 ºC	2 min
x5 cycles	94 ºC	30 sec
	72 ºC	2 min
x5 cycles	94 ºC	30 sec
	70 ºC	2 min
x25 cycles	94 ºC	30 sec
	68 ºC	30 sec
	72 ºC	2 min
	72 ºC	10 min
	15 ºC	∞

3’ RACE reaction

(Sample reaction)

5 units/μL Ex Taq	0.25 μL
10x Univrsal primer A mix (UPM) / 10 μM Nested universal primer A (NUP)	5 μL / 1 μL
10 μM st (3’RACE) primer / 10 μM st (3’RACE) nested primer	1 μL / 1 μL
3’ RACE-ready cDNA / 3’ RACE PCR (nested)	1 μL / 2 μL
miliQ	To 50 μL

(Thermal cycle setting)

	94 ºC	2 min
x5 cycles	94 ºC	30 sec
	72 ºC	2 min
x5 cycles	94 ºC	30 sec
	70 ºC	2 min
x25 cycles	94 ºC	30 sec
	68 ºC	30 sec
	72 ºC	2 min
	72 ºC	10 min
	15 ºC	∞

The amplificons were purified from an agarose gel after electrophoresis and were cloned into the pCR-Blunt II-TOPO vector and sequenced.

2.2.4 Predicting domain structures of DapmaDNMT3.1 and DapmaDNMT3.2

Gene structural and multiple sequence alignment analyses of the putative DapmaDNMT3s were conducted using the NCBI Conserved Domain Database [67] and Pfam database [68] tools and

COBALT [69]. The conserved PWWP and ADD domain sequences and catalytic domain motif sequences have been identified in previous studies [49,70,71].

2.2.5 Phylogenetic tree construction

Amino acid sequences of DNMT3s of various animal species were retrieved from NCBI (http://www.ncbi.nlm.nih.gov/) (Table 2.1).

To obtain putative DNMT3s from *Daphnia pulex*, the *D. pulex* genome database BLAST searched: (http://arthropods.eugenes.org/EvidentialGene/daphnia/daphnia_pulex/daphnia_pulex_genes2017/blast/) using the *D. magna* DNMT3 amino acid sequences as queries. Complete amino acid sequences of all proteins were used to construct a phylogenetic tree. Multiple sequence alignments were constructed using ClustalW in MEGA version 7.0. The following setting were used: pairwise alignment parameters: gap opening penalty = 6.00, gap extension penalty = 0.21, and identity protein weight; matrix multiple alignment parameters: gap opening penalty = 10.00, gap extension penalty = 0.24, delay divergent cut-off = 30%, and gap separation distance = 4 [97]. The phylogenetic tree was constructed using the p-distance algorithm and the neighbor-joining method implemented in MEGA.

Table 2.1 Gene names, species names, and GenBank accession numbers were used for the phylogenic analysis.

Gene	Species	Abbreviations	GenBank accession number
DNMT3A	*Homo sapiens*	*HsDNMT3A*	Q9Y6K1.4
DNMT3B	*Homo sapiens*	*HsDNMT3B*	Q9UBC3.1
DNMT3L	*Homo sapiens*	*HsDNMT3L*	Q9UJW3.3
DNMT3A	*Mus musculus*	*MmDNMT3A*	P13864.5
DNMT3B	*Mus musculus*	*MmDNMT3A*	O88509.2
DNMT3C	*Mus musculus*	*MmDNMT3C*	P0DOY1.2
DNMT3L	*Mus musculus*	*MmDNMT3L*	AAH83147.1
DNMT3	*Apis mellifera*	*AmDNMT3*	NP_001177350.1
DNMT3	*Nasonia vitripennis*	*NvDNMT3*	XP_008204446.1
DRM2	*Arabidopsis thaliana*	*AtDRM2*	Q9M548.1

2.2.6 Expression Analysis by RT-qPCR

DapmaDNMT3.1 and DapmaDNMT3.2 expression levels were examined in embryos, juveniles, and adults stressed by caloric restriction. First, their embryonic expression levels were analyzed using embryonic cDNAs and normalized to the number of embryos as described

previously [72]. Embryonic stages examined were 0, 3, 6, 9, 18, 36, 48, and 72 h after oviposition. Second, to examine gene expression during juvenile stages, five to ten daphniids were collected at 72 h (instar 1), 96 h (instar 2), 120 h (instar 3), 144 h (instar 4), and 192 h (instar 5). Total RNA purification and cDNA synthesis were performed as described above. qPCRs were run in three technical replicates using an SYBR GreenER qPCR SuperMix Universal Kit (Invitrogen) in an Mx3005P Real-Time PCR System (Agilent Technologies, CA, USA). Thermal cycling conditions were as follows: 2 min at 50°C and 10 min 95°C, followed by 40 cycles of 15 s at 95°C and 1 min at 60°C. Gel electrophoresis and dissociation curve analyses were performed to confirm the correct amplicon size and primer specificity [97]. Relative *DapmaDNMT* mRNA levels were normalized to *RPL32* transcript level [97]. Third, adults cultured under caloric restriction conditions were collected, as mentioned above. The following experimental steps, including Total RNA purification, cDNA synthesis, and qPCR, were performed in the same way as for gene expression analysis using juveniles. Sequences of the primers used for qPCR are shown in Table 1. Three biological replicates were used in each gene expression analysis.

2.2.7 Feeding experiment

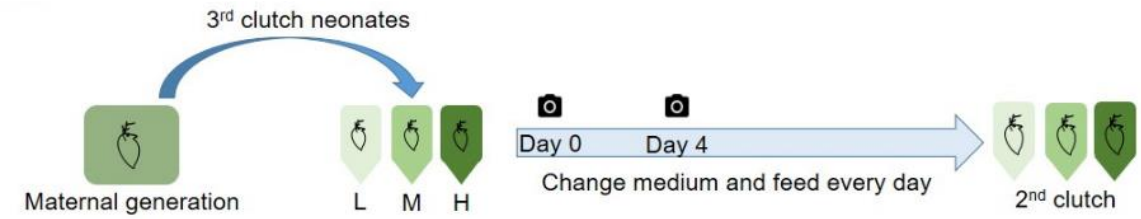

Figure 2.1 Overview of the experimental design. The green rectangle represents the 2.5-L tank for maintenance culture in the ADaM medium. The curved arrow represents the transfer of an individual neonate into a 50-mL conical tube, represented by the tube-like shape. *Chlorella vulgaris* feed levels (low (L), medium (M), and high (H)) are indicated in different shades of green. The arrow represents the cultural process. Black camera icons above the culture timeline indicate the time points at which daphniids were individually imaged to measure their body length.

Before culturing under the calorie restriction conditions, in order to control for maternal effects, 40 *Daphnia* were cultured in 2.5 L of ADaM and daily fed 1.5×10^9 cells mL^{-1} of *Chlorella* for at least three generations. Fifteen neonates from the third clutch were randomly selected and divided into three food level treatments. Each individual was transferred to a 50 mL tube containing 40 mL of ADaM and reared on high, medium, or low food levels. In the high-level food treatment, each *Daphnia* was fed 5.12×10^7 cells daily, which is 1.3 fold higher than the initial maternal condition. In the medium- and low-level food treatments, individuals were fed 8- and 32-fold lower amounts, respectively. All daphniids were cultured until they produced a second clutch (approximately day 12). For expression analysis by RT-qPCR, all five daphniids of each treatment were sampled after removing eggs from their brood chambers. During culture, the medium was changed daily, and the produced offspring were removed. Three biological replicates were used in this experiment.

2.2.8 Measuring body length and growth rate of daphnids

To examine the effect of starvation on *D. magna* growth, we measured body length from the center of the eye to the base of the tail [73]. The juvenile growth rate was calculated according to a previous study [74] based on body length on days 0 and 4, using the following formula:

$$g = \frac{lnL_{day\ 4} - lnL_{day\ 0}}{t}$$

Where g represents juvenile growth rate, L represents body length, and t is the time in days from day 0 to day 4.

2.2.9 Statistical analyses

Statistical analyses were conducted using the statistical program R, version 3.2.5. Data (juvenile growth rate, number of neonates, and relative expression) were analyzed using one-way

ANOVA and *posthoc* analysis (Tukey's honestly significant difference). The level of significance was $P < 0.05$. Data of embryonic expression were analyzed using a pairwise t-test.

2.3 Results

2.3.1 Annotation of DNMT3 orthologs in *Daphnia* genomes

First of all, I used the DNMT3 amino acid sequence of the honey bee as bait for tblastn searches to examine the existence of DNTM3 orthologs in *Daphnia.* As a result, I searched two putative orthologs of DNMT3 in both the *D.magna and D.pulex* genome database (Table 2.2).

Table 2.2 Genome annotation of *DNMT3* genes in *Daphnia* species

Species	Gene ID	Name	Scaffold	Location
Daphnia magna	*Dapma7bEVm006722t1*	*DapmaDNMT3.1*	2140	136605-141986
	Dapma7bEVm011900t1	*DapmaDNMT3.2*	2140	280312-283754
Daphnia pulex	*Daplx7pEVm007057t1*	*DpDNMT3.1*	125	378586-381303
	Daplx7pEVm003705t1	*DpDNMT3.2*	292	55726-61840

2.3.2 Molecular cloning of DapmaDnmt3.1 and DapmaDNMT3.2 genes from D.magna

The nucleotide sequence of cDNA and the deduced amino acid sequence of the putative DapmaDnmt3.1 are shown in Fig. 2.3. The obtained coding region contains a 2553 bp nucleotide sequence that encodes for 851 amino acids (Fig. 2.3).

```
1 ATGGCGAATAAAACCAGCAGAAGTGAATCGCAGGCGACAGAAAATGGCGTCGAACCAAAGAAAACATTAGCCTCTCGTAAGTTTATTCGTCTCGGTACTA
      M  A  N  K  T  S  R  S  E  S  Q  A  T  E  N  G  V  E  P  K  K  T  L  A  S  R  K  F  I  R  L  G  T
101 TGGTGTGGGCTAAGCTGGACGGCTGGCCTTGGTGGCCTGGCATTGTAGTTACGCACAACGATTGTGGGTTGCCTCCACCCAGGAAACCCACCAACTACTG
      M  V  W  A  K  L  D  G  W  P  W  W  P  G  I  V  V  T  H  N  D  C  G  L  P  P  P  R  K  P  T  N  Y
201 GGTGTACTGGTTCGGCGGCCATCAAACCGTTTCTGAGATGCCGACTGAAAAGCTTAGCGGTTTTCTGGATGATCATTTCATTCGGTTGCTTAATCAAGCC
    W  V  Y  W  F  G  G  H  Q  T  V  S  E  M  P  T  E  K  L  S  G  F  L  D  D  H  F  I  R  L  L  N  Q  A
301 CATAACAACCTCTATGAAAAAGGTGTTTTGGAGGCCCTGAGGATGTTGGCGCATAGTAAAAATCAGCCCAGACTCGTCAAACCAACGGCTGGCAAATTGA
      H  N  N  L  Y  E  K  G  V  L  E  A  L  R  M  L  A  H  S  K  N  Q  P  R  L  V  K  P  T  A  G  K  L
401 AATCGTGGGCGATTAAAATATTCTCGTCCGTAAAGGGCAACACCAATCGAGATGTTGTTCTGAACGACTTTCCAGAATGGCTGGTACGTTGCATCAGCCG
      K  S  W  A  I  K  I  F  S  S  V  K  G  N  T  N  R  D  V  V  L  N  D  F  P  E  W  L  V  R  C  I  S
501 AATTAAAGACACTAACGATAAATTAAAGAGAATTTCCAACGAGAAGAAAGAGAGTCGTCTGTCTACGTTCCAGGGTGGCCAAAAAAAGAAGGAGAAAAAG
    R  I  K  D  T  N  D  K  L  K  R  I  S  N  E  K  K  E  S  R  L  S  T  F  Q  G  G  Q  K  K  K  E  K  K
601 AAAAACAATGCCGAAGATGATGACGTCACTTATGGCCCGCGAGATTGCGATATTGCTGTTGTGGACAGAATCAAAGCTGGAACGCTGGACATGGATTACT
      K  N  N  A  E  D  D  D  V  T  Y  G  P  R  D  C  D  I  A  V  V  D  R  I  K  A  G  T  L  D  M  D  Y
701 TTTGCCTTGGTTGTCATGTCGAGATCATGGGTCCGTGCACAGAACATCCCCTCTTCCTCGGAAGTCTTTGCAATCAAGAATGCAAGAATGAACTCCTTGG
    F  C  L  G  C  H  V  E  I  M  G  P  C  T  E  H  P  L  F  L  G  S  L  C  N  Q  E  C  K  N  E  L  L  G
801 AACAAGTTACAGCGTTGGGGAGGACGATATTCACGTGGGCTGTGCCATTTGCGGTTCGACGGGAGATTGTTTAGTATGCGAAAACGGTTCCTGTTCCAGG
      T  S  Y  S  V  G  E  D  D  I  H  V  G  C  A  I  C  G  S  T  G  D  C  L  V  C  E  N  G  S  C  S  R
901 GTATACTGTTCGTATTGCGTGGAACTATTGGTGGGCGAAGGATCCATGTCGACCATTATGCAGAAGACGCCGTGGTTCTGCTTTCTCTGTGCCCATTTCG
      V  Y  C  S  Y  C  V  E  L  L  V  G  E  G  S  M  S  T  I  M  Q  K  T  P  W  F  C  F  L  C  A  H  F
1001 CTACAGAATCTCACGGCTTGCTTCAACCTCGTTCCGACTGGGCCCTTAAATTGCGGAATTTTCTACACCAGGAATTCCCACTGCAATTAAATCGGCATTT
    A  T  E  S  H  G  L  L  Q  P  R  S  D  W  A  L  K  L  R  N  F  L  H  Q  E  F  P  L  Q  L  N  R  H  L
1101 GTCTAAGAACGGACAACCCTCTCTCCGGGTCGTGGTACTCCACGACAACCTGGGCGCTGTCAATTACGCCCTGGGCTCATTACGTCTTCACCTCGACCAG
      S  K  N  G  Q  P  S  L  R  V  V  V  L  H  D  N  L  G  A  V  N  Y  A  L  G  S  L  R  L  H  L  D  Q
1201 TACATGGCATCGGACAGGTGGGAAGAGGTGTACGAACTCAATGGCGTCGATTTTGTTGTCCTGAAAAATGCCAATCAAATGAAAGACGAAGAATGGGCCA
      Y  M  A  S  D  R  W  E  E  V  Y  E  L  N  G  V  D  F  V  V  L  K  N  A  N  Q  M  K  D  E  E  W  A
1301 AACTGTGTCCTATTCACCTGCTCGTTTCTTGTCTTCCGGCCAAGAAATTCGATCCGCAACGTCATCAACCTGCCGGCCGAGAAGTGGGTAGAAGACAATT
    K  L  C  P  I  H  L  L  V  S  C  L  P  A  K  K  F  D  P  Q  R  H  Q  P  A  G  R  E  V  G  R  R  Q  F
1401 CGCCGAGGGAGAATATGGAGAGGCTTTTTTCGATTTCTTCCACATCAAAAATTGCATCGAACGTAATAATCAAGAGACTCCTCTTCTATGGGCTGTCGAA
      A  E  G  E  Y  G  E  A  F  F  D  F  F  H  I  K  N  C  I  E  R  N  N  Q  E  T  P  L  L  W  A  V  E
1501 AATGTCAGCTGTTATCACATCACCATTTCCAGGTTTCTTCAGATGGAGCCCATCATATTCGACATTAGAGACGGTCAAGGCTGCGTCAAACATCGTCTCG
      N  V  S  C  Y  H  I  T  I  S  R  F  L  Q  M  E  P  I  I  F  D  I  R  D  G  Q  G  C  V  K  H  R  L
1601 TATGGACCAATATTCCTGAACAGAATTTTAAACCGCAATTGGAACAAGTGATTAACAATGATTGTCCGTCCATTTCGAGCCTTCCGCTCAGTCGCGAACC
    V  W  T  N  I  P  E  Q  N  F  K  P  Q  L  E  Q  V  I  N  N  D  C  P  S  I  S  S  L  P  L  S  R  E  P
1701 TTTCTTCATTAAATATCCTTGGATCCTCGAAGATATTGTGGCCATTGCTCAACCTCGACCAGCCAATTGGCAGGAAAAACACGACCGGATGCTGTTCCAG
      F  F  I  K  Y  P  W  I  L  E  D  I  V  A  I  A  Q  P  R  P  A  N  W  Q  E  K  H  D  R  M  L  F  Q
1801 CGCGACACACGAAGCAAAACAAAGATAATCAAACGGCCATCCTATTTGGAACACTATTCCGTGGTCCAGCTAACCCAGAAATCTGCGAAAAAGAGAAGGA
      R  D  T  R  S  K  T  K  I  I  K  R  P  S  Y  L  E  H  Y  S  V  V  Q  L  T  Q  K  S  A  K  K  R  R
1901 AAATGGACGACGAGTTCCATCCGAATTGGAGATTACGTGAGCACGGCAACAAAGCCGAGGACACGGATGACGATCAGACGGATTACGTGGCCGCTCTGAC
    K  M  D  D  E  F  H  P  N  W  R  L  R  E  H  G  N  K  A  E  D  T  D  D  D  Q  T  D  Y  V  A  A  L  T
```

(continued on the next page)

```
2001 CAATCACGCGACCTACGCCCGTTCGCTTGGTTTCCCCGAGCCGTTTCCGGAGTTTGTGTCTCATCTGGATGAGGCGGCCGTCCAAGAAAGATTGAACCGT
       N  H  A  T  Y  A  R  S  L  G  F  P  E  P  F  P  E  F  V  S  H  L  D  E  A  A  V  Q  E  R  L  N  R
2101 AGTCTGCCCGTCTCGTTGTGGATTCATCTGTTCCAGCCGTTGTTGAAATTGGCGCGAATCGCTGAACCGGATTGTAAATCCAATACGCGTAGCCACCGTC
       S  L  P  V  S  L  W  I  H  L  F  Q  P  L  L  K  L  A  R  I  A  E  P  D  C  K  S  N  T  R  S  H  R
2201 ACTGTCATCAAAATAGTCGCAGTAGTCACGTGGGGTGCGTTGCTGTTTTCTCAAATACGATTTCGGATTCGGATAAGATCGGATGTAAGAAGGAGCCTGT
       H  C  H  Q  N  S  R  S  S  H  V  G  C  V  A  V  F  S  N  T  I  S  D  S  D  K  I  G  C  K  K  E  P  V
2301 CTCTTACTCCTCGATGACGGGGGAGATGCAGACAGAGTTTCATTCGATTCGTCCGATTCAGACGTTTCGCCAGATTCCAACGAATGTCCTCCGACGTCTT
       S  Y  S  S  M  T  G  E  M  Q  T  E  F  H  S  I  R  P  I  Q  T  F  R  Q  I  P  T  N  V  L  R  R  L
2401 CATGTTGAGGTGAAGGCGATCCTTCATTTTCGCTGGACAGTTGATGCTTCGAATGGATCTCTGCCGAATCCAACCCGCCGTGATGATGGGTCATGTGACT
       H  V  E  V  K  A  I  L  H  F  R  W  T  V  D  A  S  N  G  S  L  P  N  P  T  R  R  D  D  G  S  C  D
2501 TTCCATCGGCCCGCCAAGTGCGCAGATGGCGAGACATGCGAGAATCCAGAATC 2553
       F  P  S  A  R  Q  V  R  R  W  R  D  M  R  E  S  R  I
```

Fig 2.2 Nucleotide sequence of *DapmaDNMT3.1* cDNA and deduced amino acid sequence. Nucleotides are numbered beginning with the first nucleotide of the translational start codon.

```
   1 ATGACGACTTACGATCGCGAAGACTTTTATGACAGTGATGCTACGCAGTTCAGTGAATCCGATGATGATAACTTTGAAGGGAATTTTGGAGTTGATCCAA
       M  T  T  Y  D  R  E  D  F  Y  D  S  D  A  T  Q  F  S  E  S  D  D  D  N  F  E  G  N  F  G  V  D  P
 101 TCGATGACCTTGATCAATGGATTCCCCCTCTTTTCTATCTAGCCAAAGGTTCTCTACAGAGCATTCAGAATAACAAAAGCAGCCTGGAAAATTTTTGTTT
       I  D  D  L  D  Q  W  I  P  P  L  F  Y  L  A  K  G  S  L  Q  S  I  Q  N  N  K  S  S  L  E  N  F  C  L
 201 AGCATGTTGGGAAAAAGGAATGCATCCCCATCCGTTTTTTAACGGTGGTCTTTGCCATCCATGCAAAGAAAGATTGCTACATACAATGTTTTCAAAAAGT
       A  C  W  E  K  G  M  H  P  H  P  F  F  N  G  G  L  C  H  P  C  K  E  R  L  L  H  T  M  F  S  K  S
 301 GCAGATGGTTTTCACCTCTATTGCACTGTTTGTGGATCAAGATCAAATGCCTGTGTGAATTGCACGAGCAGCAATTGCATAAAAAAGTACTGTGTGAATT
       A  D  G  F  H  L  Y  C  T  V  C  G  S  R  S  N  A  C  V  N  C  T  S  S  N  C  I  K  K  Y  C  V  N
 401 GCCTGAATATCTGGACGGATTACAGTGACAAGCTAGTAAATAATAAATCCAATGACTGGATTTGTTTCCTTTGCCTCCCAGAACCCAATCTTTTACTGCA
       C  L  N  I  W  T  D  Y  S  D  K  L  V  N  N  K  S  N  D  W  I  C  F  L  C  L  P  E  P  N  L  L  L  Q
 501 AGCTAATCATGATTGGGCTCAAAAGGTTTTGTTCTTTCATGAACCGCTATCGGTGTATGGTCCGAGAGCTCTGTACTGGAAGAAGCAACCCTTGCGTGTT
       A  N  H  D  W  A  Q  K  V  L  F  F  H  E  P  L  S  V  Y  G  P  R  A  L  Y  W  K  K  Q  P  L  R  V
 601 TTGTCTCTCTTTGACGGAATTGGGACTGGTTTGGTGGCATTACGCAAACTGGGTATTCAAGTAGAAGTTTACTACGCCTCTGAGGTTTTGACTGCTGCGG
       L  S  L  F  D  G  I  G  T  G  L  V  A  L  R  K  L  G  I  Q  V  E  V  Y  Y  A  S  E  V  L  T  A  A
 701 CCACTGTCTCCAGGACCAGACTAGGAGGAGTGCTCCAGCACATCGGCAGCGTGGGGGAAGTAACGGAGAGGCGGCTAGAAGAGATAGCACCTATTCACCT
       A  T  V  S  R  T  R  L  G  G  V  L  Q  H  I  G  S  V  G  E  V  T  E  R  R  L  E  E  I  A  P  I  H  L
 801 GCTCATCGGGGGCTCCCCTTGCAATGATTTTAGCGCCATTAACCGATTCCCCAAAGATTTTTACGACCCAAGAGGTTATTCGAGATATTTCTTCGATTTC
       L  I  G  G  S  P  C  N  D  F  S  A  I  N  R  F  P  K  D  F  Y  D  P  R  G  Y  S  R  Y  F  F  D  F
 901 GTCCGAGTTCTGAATCTCATGCGGAAGATCAATGGGCAATATCAGCATCTACTGTGGCTCTTTGAAAATGTAGCGTCCATGCCTCAACATTATCGCGACA
       V  R  V  L  N  L  M  R  K  I  N  G  Q  Y  Q  H  L  L  W  L  F  E  N  V  A  S  M  P  Q  H  Y  R  D
1001 CAATATCCAGGCATTTGGATTGCCAGCCAGCCGTAATTGATGCCAAGAACTTCAGCCCTCAACTACGCAGACGCCTCTTTTGGGGTAACATTCCCGGGCT
       T  I  S  R  H  L  D  C  Q  P  A  V  I  D  A  K  N  F  S  P  Q  L  R  R  R  L  F  W  G  N  I  P  G  L
1101 TTTTACCGTTCACGCCGAGCAAATGACGATGGATGGGGAACCGTTGACCCTCGACAAATCTCTGATGCCTAACTCTGGTCGTAGTGCTGCCCAGGCCAAG
       F  T  V  H  A  E  Q  M  T  M  D  G  E  P  L  T  L  D  K  S  L  M  P  N  S  G  R  S  A  A  Q  A  K
```

(continued on the next page)

```
1201 ATCCGAACTCTGACGACCAACACCAATTCACTGCTGCAAGGCAGGACAGAGAACTGCAAGAGCCGAAAGGATTTGGCCTCGCTCTTTCCGGTTCGTTTCT
      I  R  T  L  T  T  N  T  N  S  L  L  Q  G  R  T  E  N  C  K  S  R  K  D  L  A  S  L  F  P  V  R  F
1301 CTTTCCAACAAGATGAACTGCGAAACGCCGATGTCGAAAGCGATGTTGCTAGACATTCGAAGAAAGGAAAAAGGGACTCCACAAGCGGCATAAATGCAAC
     S  F  Q  Q  D  E  L  R  N  A  D  V  E  S  D  V  A  R  H  S  K  K  G  K  R  D  S  T  S  G  I  N  A  T
1401 CGATAAACCTCCGCGTACGGTGGCCGATGAAGATGACAACCAGCAGACGGACGTATTGTGGCTCCAGGAAATTGAACATGTTTTTGGTCTGCCTCGCCAT
       D  K  P  P  R  T  V  A  D  E  D  D  N  Q  Q  T  D  V  L  W  L  Q  E  I  E  H  V  F  G  L  P  R  H
1501 TTTACCGATGTGGGAAACATGTCCCGCACTGATCGTCAGAAGCTTTTGGGTCACGCCTGGTCGGTTCCAGTCATCGTTTCTATTTTCTCCAATCTCAAGA
      F  T  D  V  G  N  M  S  R  T  D  R  Q  K  L  L  G  H  A  W  S  V  P  V  I  V  S  I  F  S  N  L  K
1601 GTTACACGGTTTGA 1614
     S  Y  T  V  *
```

Fig 2.3 Nucleotide sequence of *DapmaDNMT3.2* cDNA and deduced amino acid sequence. Nucleotides are numbered, beginning with the first nucleotide of the translational start codon. The asterisk indicates the translational termination codon.

To determine the full length of the cDNA sequence of *DapmaDNMT3.2.* I performed 5' and 3' RACE reactions and obtained 1614 bp nucleotide sequence encoded for 538 amino acids as showed in Fig. 2.3.

2.3.3 Domain structures of DapmaDNMT3.1 and DapmaDNMT3.2

To examine the domain structures of the *D. magna* DNMT3 orthologs, DapmaDNMT3.1 and DapmaDNMT3.2, I searched for the conserved domains ADD and PWWP, and the catalytic domain in DapmaDNMT3.1 and DapmaDNMT3.2 by comparing them with the structural domains of the *Mus musculus* (P13864.5, O88509.2, P0DOY1.2, and AAH83147.1) and *A. mellifera* (NP_001177350.1) orthologs (Fig. 2.4).

The N-terminus of DapmaDNMT3.1 harbors both the PWWP and ADD domains (Fig. 2.4 and Fig. 2.5). However, in the C-terminus, it lacks the conserved methyltransferase motifs, except motif VI, including the ENV residues, which is known in going along with PC residues of motif IV to constitute the catalytic center of mammalian DNMT3 [75] (Fig. 2.7). In contrast, DapmaDNMT3.2 has a domain organization characteristic of DNMT3 enzymes, with six

methyltransferase motifs (I, IV, VI, VIII, IX, and X) at the C-terminus and the ADD domain at the N-terminus (Figs. 2.6 and 2.7). However, it lacks the PWWP domain (Fig. 2.5).

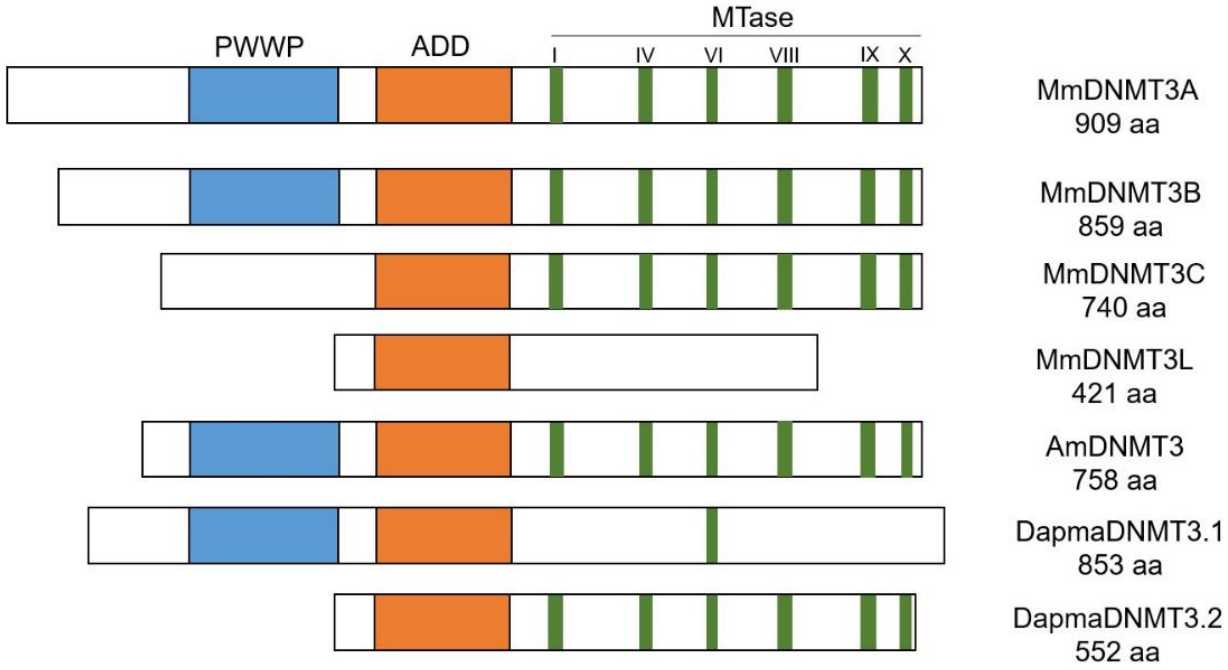

Figure 2.4 Schematic diagrams of the domain structures of DNMT3 proteins. The blue block represents the PWWP domain. The orange block represents the ADD domain. The green bars represent the conserved methyltransferase motifs in the DNMT3 proteins. Mm: *Mus musculus*, Am *Apis mellifera*.

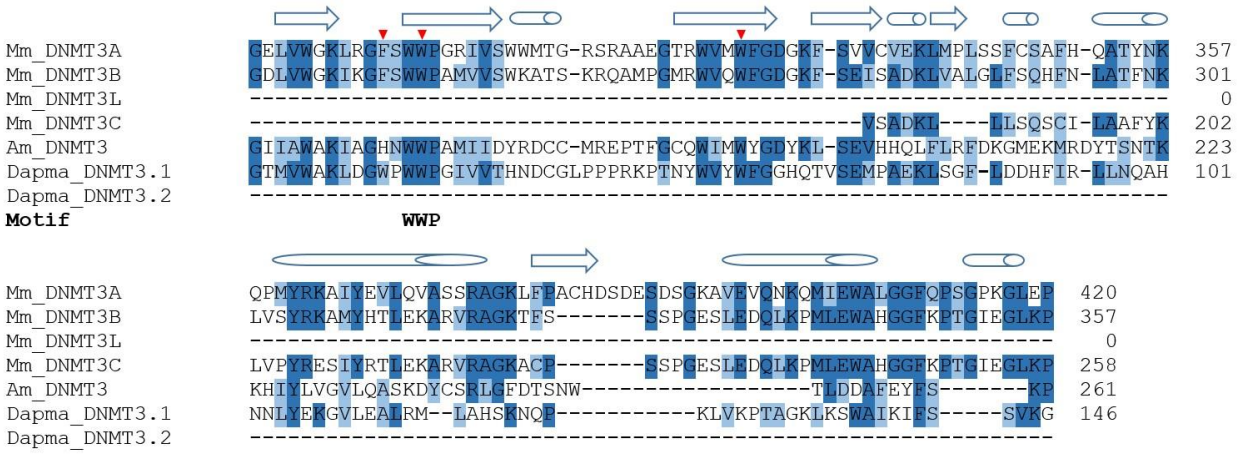

Figure 2.5 Multiple sequence alignment of DNMT3 PWWP domains. Identical residues are highlighted in dark blue and residues with similar characteristics in light blue. In each position, more than 60% of the residues are identical or similar. Dashes indicate gaps in the alignment**.** Numbers represent amino acid positions. Secondary structural elements of the mammalian DNMT3 PWWP domain [49] are shown above the sequences (arrow for β-barrel and cylinder for α-helix). Red triangles above the sequences show conserved aromatic residues. Mm: *Mus musculus*, Am *Apis mellifera*.

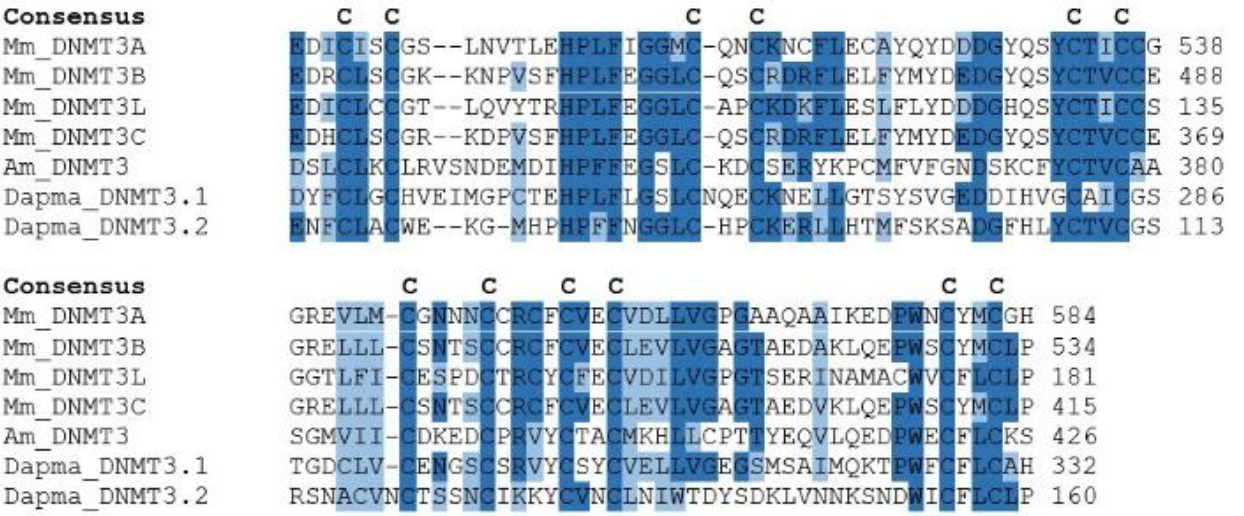

Figure 2.6 Multiple sequence alignment of DNMT3 ADD domains. Identical residues are highlighted in dark blue and residues with similar characteristics in light blue. In each position, more than 70% of the residues are identical or similar. Dashes indicate gaps in the alignment. Numbers represent amino acid positions. The consensus shows the conserved cysteine residues involved in zinc finger formation [70]. Mm: *Mus musculus* and Am: *Apis mellifera*.

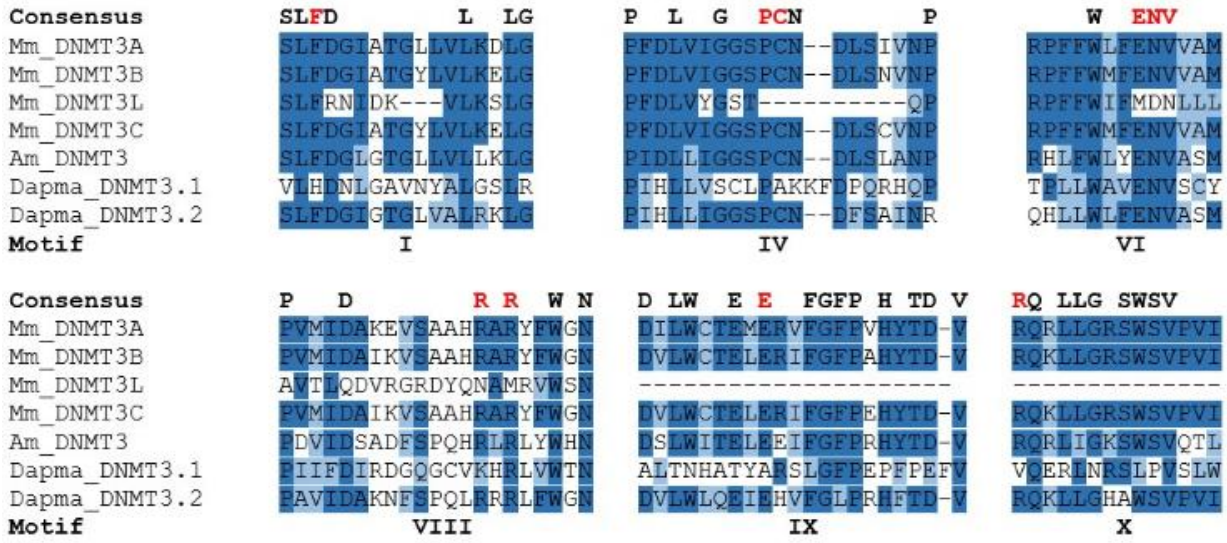

Figure 2.7 Multiple sequence alignment of key motifs in the DNMT3 catalytic domain. Identical residues are highlighted in dark blue and residues with similar characteristics in light blue. In each position, more than 70% of residues are identical or similar. The consensus shows the conserved residues (85–100%), among which functionally important residues are highlighted in red [71,76]. Mm: *Mus musculus*, Am *Apis mellifera* Roman numerals indicate the major conservative motifs of the C-terminal catalytic domain.

2.3.4 Phylogenetic relationships of DapmaDNMT3.1 and DapmaDNMT3.2

To analyze the evolutionary relationships of DapmaDNMT3.1 and DapmaDNMT3.2, I constructed a phylogenetic tree with amino acid sequences of mammalian, insect, and *D. pulex* orthologs. The two DapmaDNMT3s were clustered with insect DNMT3 proteins, which is in good agreement with the taxonomic relationship between these groups. Noticeably, DNMT3.1 proteins in *Daphnia* species were not grouped into a cluster, including insect DNMT3s and *Daphnia* DNMT3.2 (Fig. 2.8).

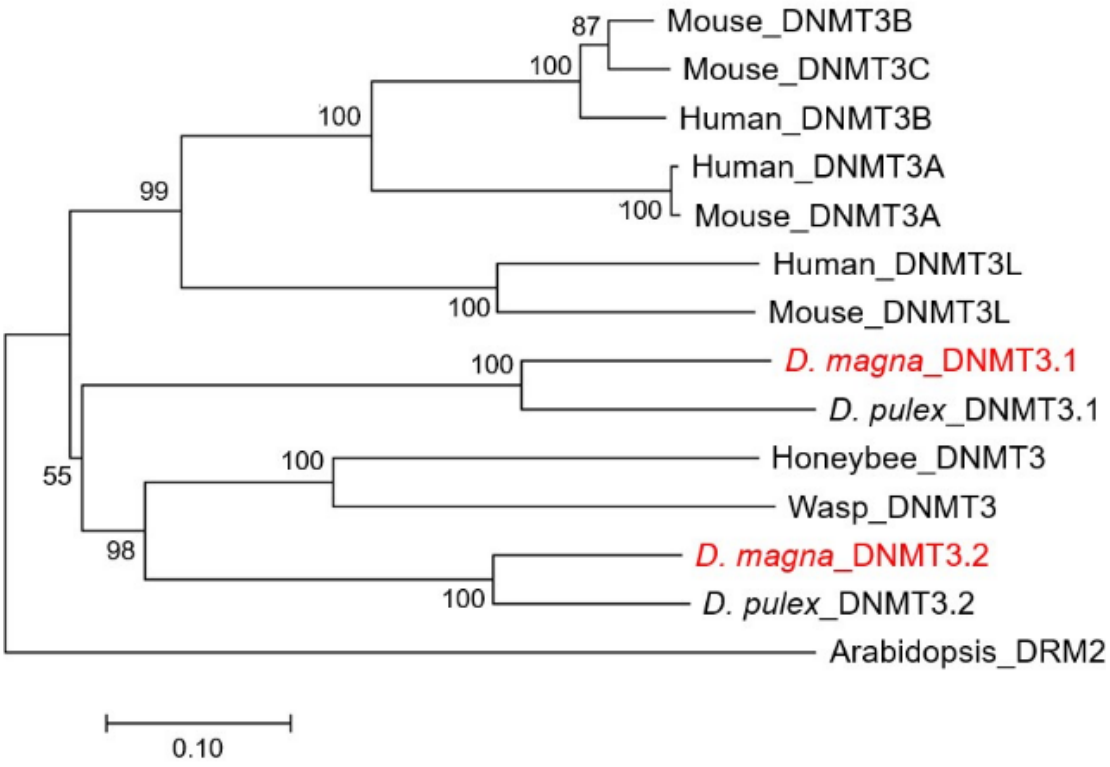

Figure 2.8 Phylogenetic relationships between DNMT3s in *Daphnia sp.* and other species. The percentages of the replicate tree in which the associated taxa clustered together in the bootstrap test (1,000 replicates) are shown next to the branches. The tree was rooted using the DNMT DRM2 of *Arabidopsis thaliana.* The bar indicates branch length and corresponds to the mean number of differences ($P < 0.1$) per residue along each branch. Evolutionary distances were computed using the p-distance method. Accession numbers of all proteins are listed in Table 2.1

2.3.5 Temporal expression of *DapmaDNMT3s* during embryonic development

To evaluate the roles of *DapmaDNMT3.1* and *DapmaDNMT3.2* in development, I examined the temporal mRNA expression of *DapmaDNMT3s* at various developmental stages of parthenogenetic females (0–72 h after oviposition for embryonic stages and 72–192 h after oviposition for juvenile stages) using quantitative reverse-transcription RT-PCR.

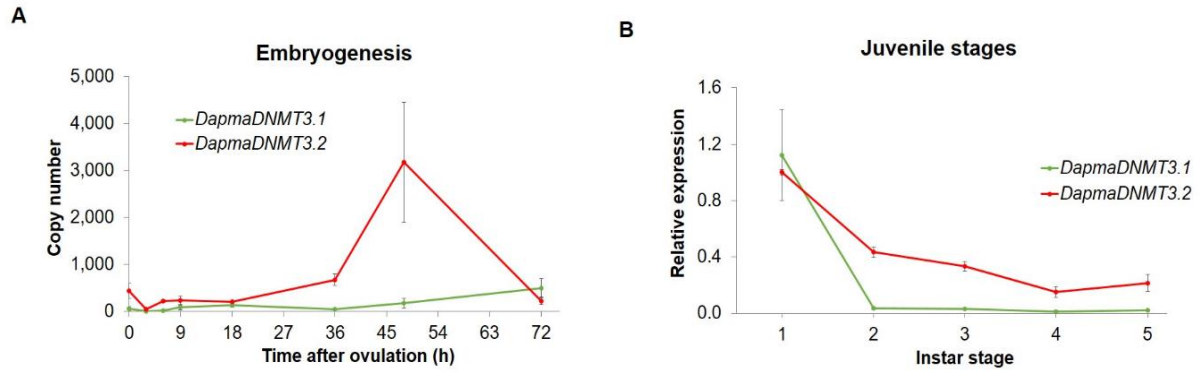

Figure 2.9 Temporal expression profiles of the *DapmaDNMT3* genes during embryogenesis and juvenile stages. (A) Expression levels of *DapmaDNMT3.1* and *DapmaDNMT3.2* during embryogenesis. Embryonic development was staged at 0 h (single-cell stage), 3 h (blastulation stage), 6 h (gastrulation stage), 9 h (neurulation stage), 18 h (early thoracic appendage-developing stage), 36 h (middle carapace-developing stage), 48 h (further developed thoracic appendages and antennae embryo), 72 h (juvenile instar 1). Results are shown as copy numbers of transcripts per egg and represent the mean ± standard error of the mean (SEM) of three independent biological replicates. (B) Relative expression levels of the two *DapmaDNMT3s* during juvenile stages. Juveniles were cultured under nutrient-rich conditions. Expression was normalized to ribosomal protein L32 gene (*RPL32*) expression. Data are the mean ± SEM of three independent biological replicates.

Compared to *DapmaDNMT3.1* expression, *DapmaDNMT3.2* expression changed more significantly in a stage-dependent manner (Fig 2.9A). Maternal *DapmaDNMT3.2* transcripts were present at 0 h (single-cell stage), but significantly decreased at 3 h (p = 0.0046) (blastula stage) and remained low until 18 h. *DapmaDNMT3.2* expression increased as of 36 h (p = 0.0012 compared to 18 h) and peaked at 48 h. *DapmaDNMT3.1* transcript levels were relatively low during embryogenesis but increased toward completion of embryogenesis at 72 h since 36 h (p = 0.0082), which corresponds with the first instar stage (Fig 2.9A). In the juvenile stages (first to fifth instar stages) under nutrient-rich conditions, both genes were downregulated, with *DapmaDNMT3.1* being the most strongly downregulated (Fig 2.9B).

2.3.6 Caloric restriction upregulates *DapmaDNMT3.1* expression

Among the environmental cues that are known to affect DNA methylation in *D. magna* [62–65], in this study, we chose caloric restriction [65] and examined its effect on the expression of *DapmaDNMT3.1* and *DapmaDNMT3.2*.

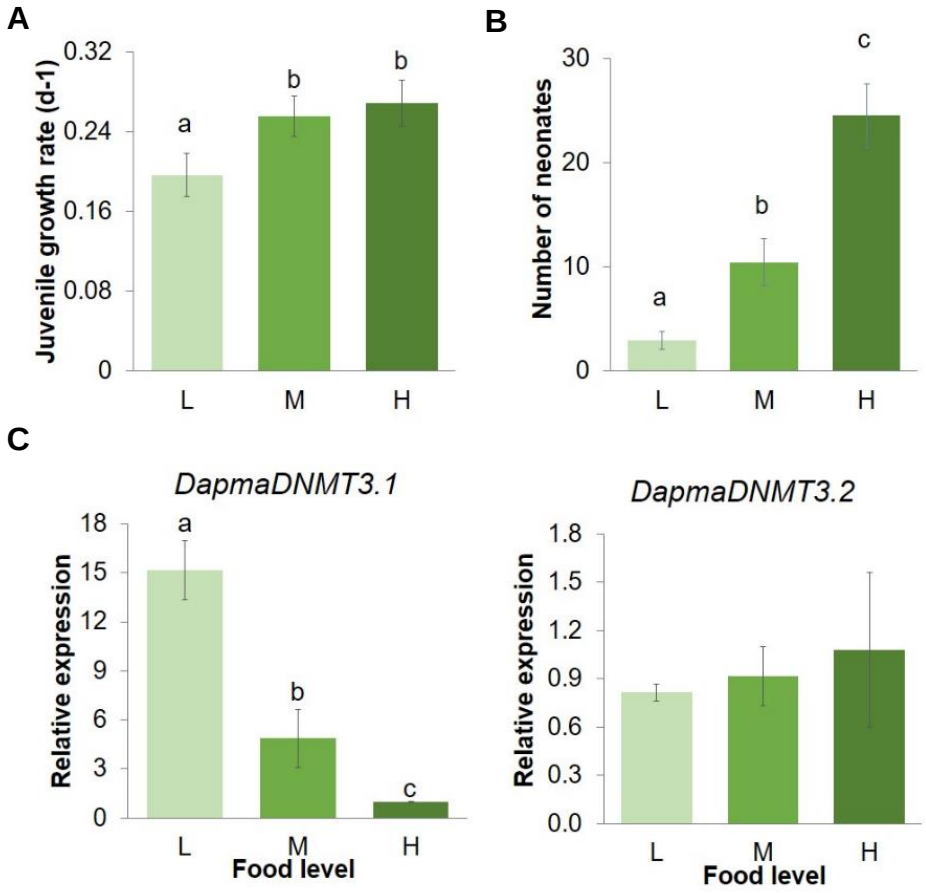

Figure 2.10 Phenotype and *DapmaDNMT3* expression in response to caloric restriction. (A) The juvenile growth rate of the daphniids from day 0 to day 4. (B) The number of neonates in the second clutch. Error bars indicate the standard deviation of the mean (n = 15). (C) Relative expression of *DapmaDNMT3.1* and *DapmaDNMT3.2* in 12-day adults fed at the three feed levels. Data are the mean fold change from the calibrator group (H). Expression was normalized to *RPL32* expression. Error bars indicate the standard deviation of the mean (n = 3). Different letters indicate a significant difference (Tukey's honestly significant difference tests after one-way ANOVA, $p < 0.05$).

To determine food levels at which the growth rate and fecundity rates would be reduced, we fed *D. magna Chlorella vulgaris* algae at three feed levels, 5.12×10^7 cells/daphniid (High), 6.4×10^6 cells/daphniid (Medium), and 1.6×10^6 cells/daphniid (Low), until they produced second clutch (Fig 2.10A). At the high feed level, the growth rate was 0.27 (± 0.02) day^{-1} and the number of neonates in the second clutch was 25 (± 3) (Figs 2.10B, C). When the amount of feed was reduced by 32-fold (low level), the growth rate significantly decreased ($p < 0.001$) (Fig 2.10B). In addition, the number of second-clutch offspring declined ($p < 0.001$) since 8-fold reduction (medium level) (Fig 2.10C). These results demonstrated food restriction affects the growth rate and clutch size in *Daphnia*. Thus, we used these food levels to analyze the effect of caloric restriction on *DapmaDNMT3* expression at the second clutch stage. *DapmaDNMT3.1* expression was upregulated by 4.8 (± 1.7) ($p = 0.03$) and 15 (± 1.8) ($p < 0.001$) fold in animals fed medium and low feed levels, respectively as compared to those fed the high food level (Fig 2.10C). In contrast, the expression of *DapmaDNMT3.2* did not show a significant difference in medium and low levels, $p = 0.78$ and 0.55, respectively (Fig 2.10).

2.4 Discussion

In this study, we first analyzed the domain organization of DapmaDNMT3.1 and DapmaDNMT3.2. DapmaDNMT3.2 has six methyltransferase motifs (I, IV, VI, VIII, IX, and X) in its C-terminus and an N-terminal ADD domain (Fig 2.4). However, it lacks the PWWP domain, through which DNMT3 proteins recognize H3K36 trimethylation (H3K36me3) (Dhayalan et al., 2010) (Fig 2.4). A similar domain organization is found in mammalian DNMT3C, which retains enzymatically active DNMT3 family members [77]. This finding suggests that DapmaDNMT3.2 functions in DNA methylation in *D. magna*. In contrast, DapmaDNMT3.1 lacks conserved methyltransferase motifs in the C-terminal region (Fig. 2.7). Interestingly, it has a PWWP domain,

which possesses well-conserved sequences in the N-terminal β-barrel region. This is consistent with the structure of other Royal superfamily members [76]. We found three conserved aromatic residues at similar positions in other mammalian PWWP domains (Fig. 2.5), which can bind lysine-methylated histones [78]. This domain is rich in basic amino acids and has an isoelectric point of 9.63. These findings indicate that the PWWP domain of DapmaDNMT3.1 is functional and has DNA-binding ability [79]. Together with the PWWP domain, the ADD domain might mediate interactions with other proteins to direct DNA methylation [52]. Although we did not perform DNA methyltransferase activity assays, based on its domain structure, we suggest that DapmaDNMT3.1 may not only methylate DNA substrates but also serve as a regulator of the DNMT3.2-dependent *de novo* methylation machinery, as reported for mammalian DNMT3L lacking the catalytic domain [17,80]. Phylogenetic analysis indicated that DapmaDNMT3.1 had evolved uniquely in *Daphnia* species (Fig. 2.8). Future studies will have to elucidate the evolution of DNMT3.1-like proteins in closely related crustaceans and other arthropod species.

We also profiled the expression of *DapmaDNMT3.1* and *DapmaDNMT3.2* in early development and a stress condition. During embryogenesis, compared to *DapmaDNMT3.1*, *DapmaDNMT3.2* was more highly expressed in the one cell-stage and at 48 h post-ovulation, when tissue differentiation and carapace development occur. In juvenile stages, *DapmaDNMT3.2*, and especially, *DapmaDNMT3.1* were downregulated. These results suggest that DNMT3.2 may play an important role in specific developmental processes, possibly via *de novo* methylation. Interestingly, *DapmaDNMT3.1* was upregulated in response to caloric restriction. A recent study reported hypermethylation in approximately 100 genomic regions under caloric restriction in *D. magna* [65]. As DapmaDNMT3.2 is constitutively expressed after embryogenesis, even under starvation conditions, DapmaDNMT3.1 may form a heterodimer with this paralog that functions

in hypermethylation. In addition, the lower expression level of DapmaDNMT3.2 may suggest that this protein has a longer half-live than DapmaDNMT3.1. Further study of this enzyme, for example, through knockout, is necessary to understand the relationship between *DapmaDNMT3.1* activation and the modified DNA methylation pattern under caloric restriction. Phylogenetic analysis indicated that DapmaDNMT3.1 had evolved uniquely in *Daphnia* species (Fig 2.8). Future studies will have to elucidate the evolution of DNMT3.1-like proteins in closely related crustaceans and other arthropod species.

Given the fact that *DapmaDNMT3.1* expression was upregulated at the low food level, we hypothesized that Forkhead box O (FOXO), a transcription factor, may regulate the expression of *DapmaDNMT3.1* because this protein is activated under starvation and orchestrates diverse gene expression to regulate homeostasis in response to starvation [81]. In insects, FOXO also serves as a nutrition-dependent growth regulator [82]. FOXO binds to the consensus sequence G(T/A)AAA(C/T)AA [83,84]. Therefore, we searched for this sequence in the *DNMT3* promoters in *D. magna* as well as in *D. pulex.* We found a candidate FOXO-binding site only in the *DNMT3.1* promoter region in both *D. magna* and in *D. pulex* (Fig 2.11).

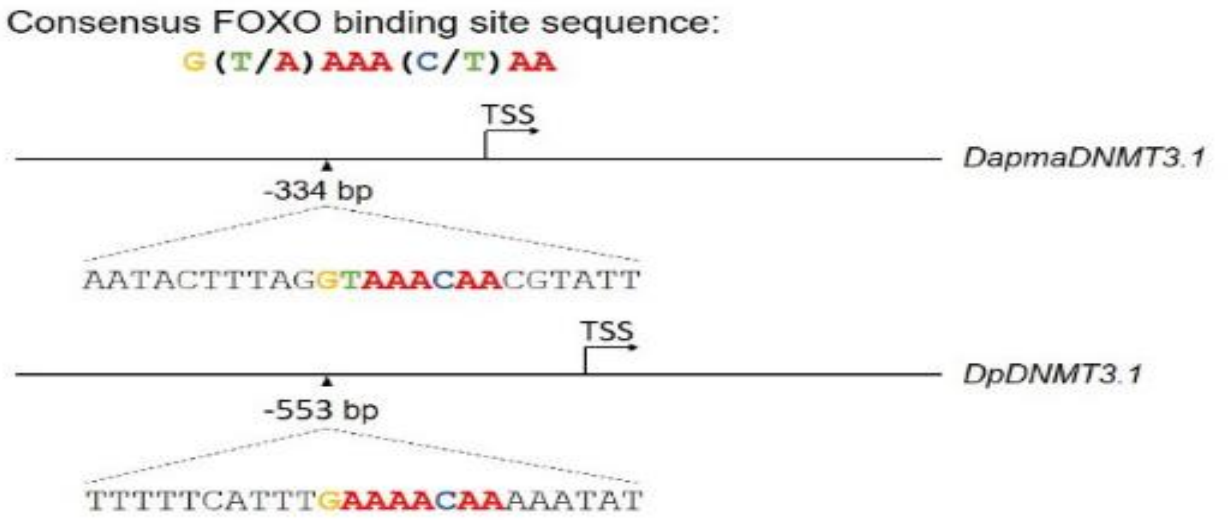

Figure 2.11 Candidate FOXO-binding site in the *DNMT3.1* promoter. The black lines indicate the genome sequences of *DapmaDNMT3.1* (*Dapma7bEVm006722t1*) and *DappuDNMT3.1* (*Daplx7pEVm007057t1*), and arrows show the transcription start sites (TSSs). The filled black triangle and numbers represent the distance between the candidate FOXO binding site (indicated in a colored font in the sequence) and the TSS.

Chapter 3

DNMT3.1 controls life span and a trade-off between growth and fecundity under the starved condition

3.1 Introduction

DNA (cytosine-5) methyltransferases (DNMT; EC 2.1.1.37) are the enzymes that catalyze the DNA methylation and generate 5-methylcytosines (5mCs) to regulate gene expression [13]. There are at least three functional orthologs, DNMT1, DNMT3A, and DNMT3B. DNMT1 maintains DNA methylation patterns after DNA replication, while DNMT3A and DNMT3B establish new methylation by using unmethylated DNA as their templates[13]. *De novo* methylation by the DNMT3 family is necessary for spatio-temporal gene expression guiding cell differentiation and organogenesis in mouse embryos [85,86]. It is also required for phenotypic changes in response to environmental stimuli [21,45,87]. In mice, homozygous mutants of *DNMT3A* resulted in multiple organ defects and lethality several weeks after birth [88]. Disruption of *DNMT3B* led to embryonic lethality [88]. DNMT3 orthologs harboring the mammalian DNMT3A/B-like domain structure are widely distributed in the animal kingdom[89]. In contrast to vertebrate genomes in which more than 80% of CpG dinucleotides are methylated, invertebrate genomes are sparsely methylated [90,91]. Functional analyses of DNMT3 have been performed only in two social insects by RNA interference [21,92,93], but both knockdown experiments did not lead to embryonic lethal phenotypes. However, in the honeybee (*Apis mellifera*), silencing of DNMT3 altered workers-destined larvae's developmental fate towards queen-like traits [21].

D. magna has the two DNMT3 orthologs [94], DapmaDNMT3a.1 (*Dapma7bEVm011900t1*) and DapmaDNMT3a.2 (*Dapma7bEVm006722t1*). DapmaDNMT3a.1 lacks the PWWP domain,

and DapmaDNMT3a.2 has the diverged methyltransferase (MTase) domain [43]. Because both of the domains are essential for DNMT3A function, we had renamed DapmaDNMT3a.2 and DapmaDNMT3a.1 as DNMT3.1 and DNMT3.2 [43]. Previously, we had found upregulation of DNMT3.1 expression in response to starvation [95], suggesting that *DNMT3.1* may play an important role under caloric restriction. To further investigate the functions of DNMT3.1 under this condition, we silenced DNMT3.1 by CRISPR/Cas-mediated mutagenesis. Phenotypic analyses of this biallelic mutant demonstrated that DNMT3.1 controls life span and the trade-off between reproduction and growth only when reproduction and growth compete.

3.2 Materials and Methods

3.2.1 Maintenance of *D. magna* strain and the DNMT3.1 mutant.

The *Daphnia magna* strain (NIES clone) was obtained from the National Institute for Environmental Studies (NIES; Tsukuba, Japan) and cultured under laboratory conditions for many generations by using ADaM as the culture medium [66]. Briefly, for maintenance of this strain, 80 individuals were cultured in the 5 liters ADaM medium and daily fed with 160 μl of 7×10^9 cells ml^{-1} *Chlorella* (*Chlorella vulgaris*) algae. The mutant line was maintained similarly by culturing 40 individuals in 2.5 liters ADaM medium and daily feeding with 80 μl of 7×10^9 cells ml^{-1} *Chlorella* (*Chlorella vulgaris*) algae. These cultures were performed at 22-24^{o}C, under a light/dark photoperiod of 16/8 h.

3.2.2 CRISPR/Cas9-mediated mutagenesis.

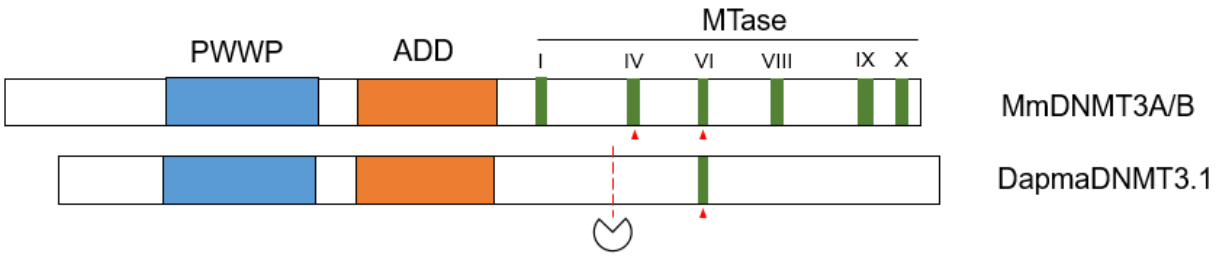

Figure 3.1 CRISPR/Cas-mediated mutagenesis of *DNMT3.1* Schematic diagrams of domain structures of DapmaDNMT3.1 and DNM3A/B of mouse (Mm = *Mus musculus*). Red triangles indicate the active sites of catalysis. The Red dashed line indicates a targeted disrupting site by CRISPR/Cas system (pie icon).

Impairment of the DNMT3.1 gene was done with CRISPR/Cas9 technology by introducing a frameshift and premature STOP codon as described previously [31]. For the preparation of the *DNMT3.1*-targeting Cas9 RNPs, we purified Cas9 proteins as described elsewhere [96]. For the synthesis of the gRNA, DNA templates with the T7 promoter and target site (5´-GGAAGAGGTGTACGAACTCAAtgg-3´, protospacer adjacent motif shown in lowercase), was amplified by PCR [31] and purified by phenol/chloroform extraction. These DNA fragments were used as templates for *in vitro* transcription with mMessage mMachine T7 Kit (Life Technologies, California, USA), followed by column purification with miniQuick Spin RNA columns (Roche diagnostics GmbH, Mannheim, Germany), phenol/chloroform extraction, ethanol precipitation, and reconstitution in DNase/RNase-free water (Life Technologies, California, USA). We incubated 2 μM gRNA with 1 μM Cas9 protein to generate Cas9 RNPs and injected them into parthenogenetic female eggs according to established procedures [97]. Accordingly, the eggs were collected from 2-3 weeks daphnids after ovulation and placed in an ice-chilled M4 medium containing 80 mM sucrose (M4-sucrose). Approximately 0.2 nL volumes of the generated Cas9 RNPs were injected using N_2 gas pressure through a glass needle. After injection, to investigate

the Cas9-induced mutations, G2 offspring were homogenized in 90 μL of 50 mM NaOH with zirconia beads. The lysate was heated at 95°C for 10 min and then neutralized with 10 μL of 1 mM Tris-HCl (pH 7.5). This crude DNA extract was centrifuged at 12,000 rpm for 5 min and then used as a template in genomic PCR. The targeted genomic regions in the *DNMT3.1* locus were amplified by PCR with Ex Taq Hot Start Version (Takara, Japan) and the following primers;

DNMT3.1-U-gD*NA* 5'-TCCGGGTCGTGGTACTCC-3'

DNMT3.1-D-gD*NA* 5'-AGACAAGAAACGAGCAGGTGAATAG-3'.

The PCR products were analyzed by polyacrylamide gel electrophoresis and DNA sequencing.

3.2.3 Culture of *D. magna* under nutrient-rich and starved conditions.

Before culturing under starved conditions, in order to control for maternal effects, 40 *Daphnia* of each line were cultured in 2.5 liters ADaM medium and daily fed with 1.5×10^9 cells ml^{-1} *Chlorella* algae for at least three generations. Neonates from the third clutch were randomly assigned, transferred individually to a 50 ml conical tube containing 40 ml ADaM medium, and subjected to nutrient-rich or starved treatments. Under the nutrient-rich condition, 5.12×10^7 cells were given to each daphnid daily. For starvation, daphnids were fed with 8-fold lower amounts of the algae. During culture, the medium was changed every day in order to avoid carbon (detrital) accumulation that could differentially affect resource availability. For life-history traits observation, 15 and 20 neonates were randomly collected from culture under nutrient-rich and starved conditions, respectively. Under the nutrient-rich condition, daphnids' body length was measured on days 0, 4, 7, and 14. The clutch size was recorded by counting the number of offspring produced from the 1st to 3rd clutch.

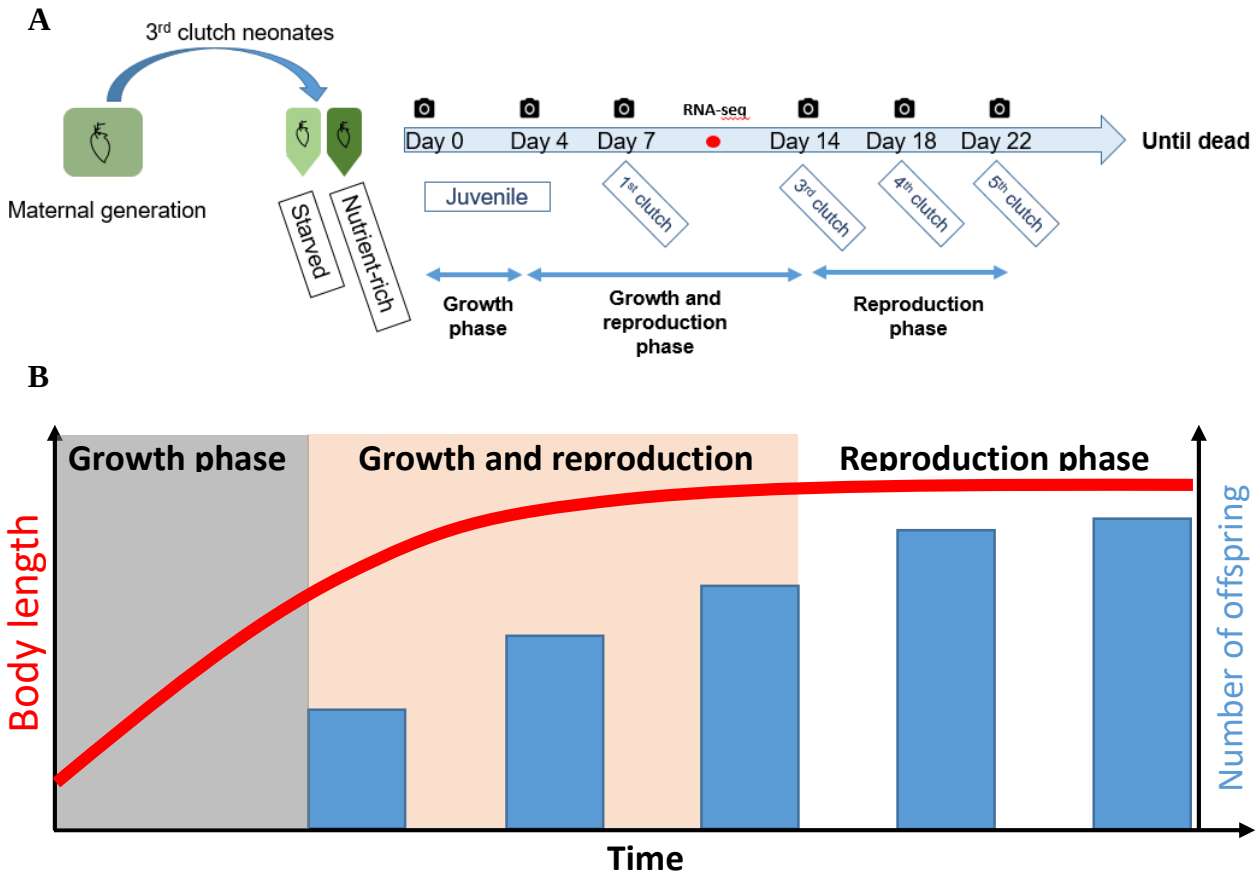

Figure 3.2 (A) Overview of the experimental design. The green rectangle represents the 2.5-L tank for maintenance culture in the ADaM medium. The curved arrow represents the transfer of an individual neonate into a 50-mL conical tube, represented by the tube-like shape. The arrow represents the cultural process. Black camera icons above the culture timeline indicate the time points at which daphniids were individually imaged to measure their body length. The red dot indicates the time point of daphnids collection for RNA seq. **(B) The graph illustrates the developmental phases of *D. magna*.** The growth curve of daphnids (solid red line) based on their body lengths and blue bars indicate the number of offspring produced. During the juvenile stage, daphnid only increases its body length (the growth phase in grey shading). After maturation, besides increasing the body length, the daphnid starts its reproduction (the growth and reproduction phase in light red shading). Moreover, later on, after reaching a maximum body length, the growth stopped and remained only reproduction activity in daphnid (the reproduction phase).

During culturing, due to handling, one wild type and one mutant were killed. Therefore, we recorded the life span of 14 individuals of wild types and mutants. For starvation experiments, the body length of daphnids was measured at the two more time points, day 18 and day 22, in addition to day 0, 4, 7, and 14. Clutch size was recorded from 1st to 5th clutch. In this treatment, we could record the life span of 20 individuals, both from wild types and mutants. For expression analysis by quantitative real-time PCR and RNA-seq, five daphnids were also cultured individually in each condition until producing 2nd clutch (day 12). Eggs were removed before homogenization for RNA extraction. Each treatment was repeated three times for triplicates of sampling.

3.2.4 Body length and growth rate analysis.

To examine the effect of starvation on *D. magna* growth, we measured body length from the center of the eye to the base of the tail [73] using a microscope and the ImageJ software (http://rsb.info.nih.gov/ij/). The growth rates of juvenile and adult daphnids were determined by using their body length on day 0 to day 4 and day 4 to day 14, respectively, and calculated as

$$g = \frac{lnL_1 - lnL_0}{t}$$

According to a previous study, where L_1 and L_0 are the final and the initial body lengths, respectively, and t is the time in days from the first to final observation[74].

3.2.5 RNA extraction and cDNA synthesis.

To extract total RNA, five female adult daphnids were collected and briefly washed. Homogenization was performed with beads using a Micro Smash machine MS-100 (TOMY; Tokyo, Japan), in the presence of Sepasol-RNA I reagent (Nacalai Tesque Inc.; Kyoto, Japan). Total RNA was isolated according to the manufacturer's protocol, which was followed by phenol/chloroform extraction. One μg of purified total RNA was converted into the first-strand

cDNA with PrimeScript II Reverse Transcriptase (Takara, Japan) and random primers (Invitrogen, Carlsbad, CA, USA) according to the manufacturer's recommended protocol.

3.2.6 Expression Analysis by Quantitative Real-Time PCR.

Total RNA purification and cDNA synthesis in adult samples treated with different food levels were performed as described above. PCR was performed using a Power SYBR Green PCR Master Mix (Thermo Fisher Scientific, USA) with Mx3005P Real-Time PCR System (Agilent Technologies; CA, USA). In the presence of the appropriate primer pairs, real-time PCR amplifications were performed in triplicate at the following conditions: 2 min at 50^{o}C and 10 min 95^{o}C, followed by 40 cycles of 15 s at 95^{o}C and 1 min at 60^{o}C. Gel electrophoresis and dissociation curve analyses were performed to confirm the correct amplicon size and the absence of non-specific bands. The relative mRNA levels of juvenile samples and adult samples treated by different food levels were analyzed by normalization of the *DapmaDNMTs* transcript level to the transcript level of ribosomal protein L32 [98]. The oligonucleotide sequences for qRT-PCR were used by the previous study [95] and combined with *DapmaDNMT1* primers *(DapmaDNMT1*-forward 5'- GAAGATTCCCTTCTGCGCTATG -3' *and DapmaDNMT1*-reverse 5'- CACGGGCTGAGAATAAGTGGT -3').

3.2.7 RNA sequencing.

Nine total RNA samples were extracted from triplicate samples of each of the three treatments (wild types in starved condition and mutants either nutrient-rich or starved condition) were used for RNA-seq provided by Novogene service (Novogene (HK) Company Limited, based on Illumina NovaSeq platforms with paired-end 150 bp sequencing strategy (en.novogene.com). Before proceeding with the sequencing, all nine samples passed the company's QC Criteria and met the library construction requirement. A summary of counted reads and percentage of total

reads mapped is shown in Table 3.1. In general, we obtained between 20 and 26 million reads for each sample, and approximately 80% of reads could be mapped to a reference genome in *D. magna*, which is available from wFleaBase.org [99].

Table 3.1. Summary of RNA-Seq reads

Line	Condition	Replicate	Number of reads	% of total mapped
Wild type	Starved	1	20,708,586	82.85
		2	21,726,268	80.03
		3	22,470,222	83.00
DNMT3.1$^{-/-}$	Nutrient rich	1	24,195,222	80.14
		2	25,194,166	80.48
		3	23,052,612	80.93
DNMT3.1$^{-/-}$	Starved	1	21,132,788	82.33
		2	26,078,976	82.14
		3	22,874,240	82.66

3.2.8 RNA-Seq Data Analysis.

Sequencing data from 9 libraries of the above samples were analyzed using CLC Genomics Workbench 12 (Qiagen) (accession number: GSE158129). The other three libraries of the triplicates from wild type in nutrient-rich condition (accession number: GSE150821) had been prepared and sequenced elsewhere by the same methods, including Daphnia culturing condition as in this study [100]. The *Daphnia magna* genome that is available from wFleaBase.org [99] was used as a reference for mapping the reads. Mapping options were set at mismatch cost 2, insertion cost 3, depletion cost 3, length fraction 0.8, and similarity fraction 0.8, expression value set to total counts. Differential expression analysis was performed with the 'Transcriptomics Analysis' toolbox and comprised 'experimental set-up,' where treatment pairs were analyzed with the option 'All group pairs.' This setting uses the Wald test and reports each gene's expression mean with a fold change between the treatment pair. Expression values were normalized using the options 'by

totals' and 'state numbers in reading 1,000,000'. The normalized values were transformed using the "Add a Constant" set at the value '1'. In order to identify the differential expressed genes (DEGs) between a pair of treatments, Anova and Likelihood ratio test were performed on the transformed values for each mapped gene, and DEGs were filtered based on false discovery rate (FDR) *p*-value cutoff FDR $p \leq 0.05$ and fold change cutoff FC $\geq |1.5|$. k-Means clustering was performed by iDEP(v.9) [101]. A list of gene ID of DEGs merged counts was uploaded to iDEP, and parameters for analysis were set following a previous study [102]. Accordingly, counts were filtered out by criteria of at least 0.5 counts per million in one of the samples and transformed by VST (variance stabilizing transform). Heatmap was visualized by a blue-white-red color scheme, and k-Means was clustered for all of the filtered genes by choosing 5 clusters. The Daphnia magna genome's gene ID was annotated by NCBI homologs using Blast2GO features within OmicsBox 1.2.4 [103]. The annotated genes in each cluster were examined for the enrichment of GO terms within the subsets of the assembled sequences via Fisher's Exact Test executed within OmicsBox 1.2.4 [104].

3.2.9 Statistics.

Statistical analyses were conducted using statistical program R version 3.2.5. Growth rate, clutch size, and median lifespan were analyzed by pairwise t-test and Student's t-test with Welch's correction. The "FSA" R package performed fitted von Bertalanffy growth. The "survival" R package performed Kaplan Meier survival curves and log-rank test analysis. Two-way ANOVA and Fisher's LSD test were performed by "agricolae" R package. The level of significance was $P < 0.05$.

3.3 Results

3.3.1 CRISPR/Cas-mediated mutagenesis of *DNMT3.1*.

To investigate the functions of *DNMT3.1* in *D. magna*, we attempted to mutate this gene using the CRISPR/Cas system. As with the DNMT3L in mammals, DNMT3.1 lacks five out of six characteristic motifs of the MTase domain in catalytically active DNMT3 proteins except motif VI (Fig. 2.4) [95]. gRNA was designed to bind upstream of the motif VI because the diverged MTase domain of DNMT3.1 may interact with another *D. magna* DNMT3 ortholog DNMT3.2 harboring all of the six motifs for *de novo* methylation as well as the interaction between DNMT3L and DNMT3A in mammals[105]. Besides, truncation of the C-terminus of DNMT3A/B led to a significant decrease of their protein levels in human embryonic stem cells [106]. There are more than six base pair mismatches between this gRNA and the other D. magna DNMT genes (Fig. 3.3). This specificity of the gRNA to *DNMT3.1* could avoid off-target effects to the other *DNMT* genes because the DNA region with up to five base pair mismatches with gRNA is susceptible to editing by Cas9/gRNA complex[107,108].

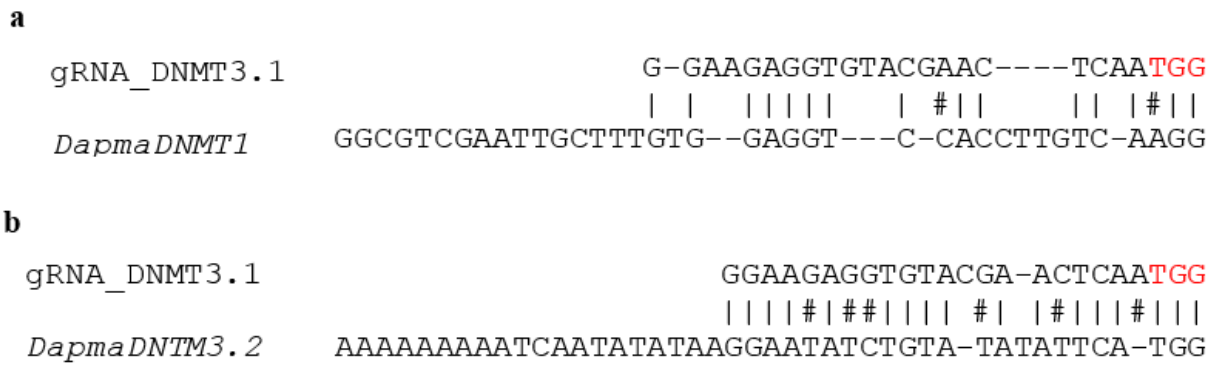

Figure 3.3 Nucleotide sequences alignment of gRNA_DNMT3.1 against *DNMT* genes in *Daphnia magna* genome. Dash indicates a gap in the alignment. The vertical bar indicates a match. Hashtag indicates a mismatch. The PAM site in the genomic sequences is highlighted in red text. (**a)** The alignment shows 12 gaps and 2 mismatches between the gRNA_DNMT3.1 and the genome sequence of *DNMT1 (Dapma7bEVm005001t1).* (**b**) The alignment shows 6 mismatches and 3 gaps between the gRNA_DNMT3.1 and the genome sequence of *DNMT3.2 (Dapma7bEVm011900t1).*

We injected Cas9 ribonucleoproteins (RNPs) comprising the purified Cas9 proteins and targeting gRNA into 48 parthenogenetic female eggs, of which 15 survived until the adult stage. G2 progenies of these potential founder lines were used for genotyping. We cloned and sequenced genomic PCR products encompassing the gRNA-targeted site to find mutant lines. Of the 15, we found one founder animal that produced offspring harboring biallelic indel mutations around the targeted site (Fig. 3.4). This line's biallelic indel mutations led to frameshifts, resulting in premature STOP codons occurring in both alleles (Fig. 3.4). We named this mutant line *DNMT3.1*$^{-/-}$ and used it for phenotyping and transcriptional analysis.

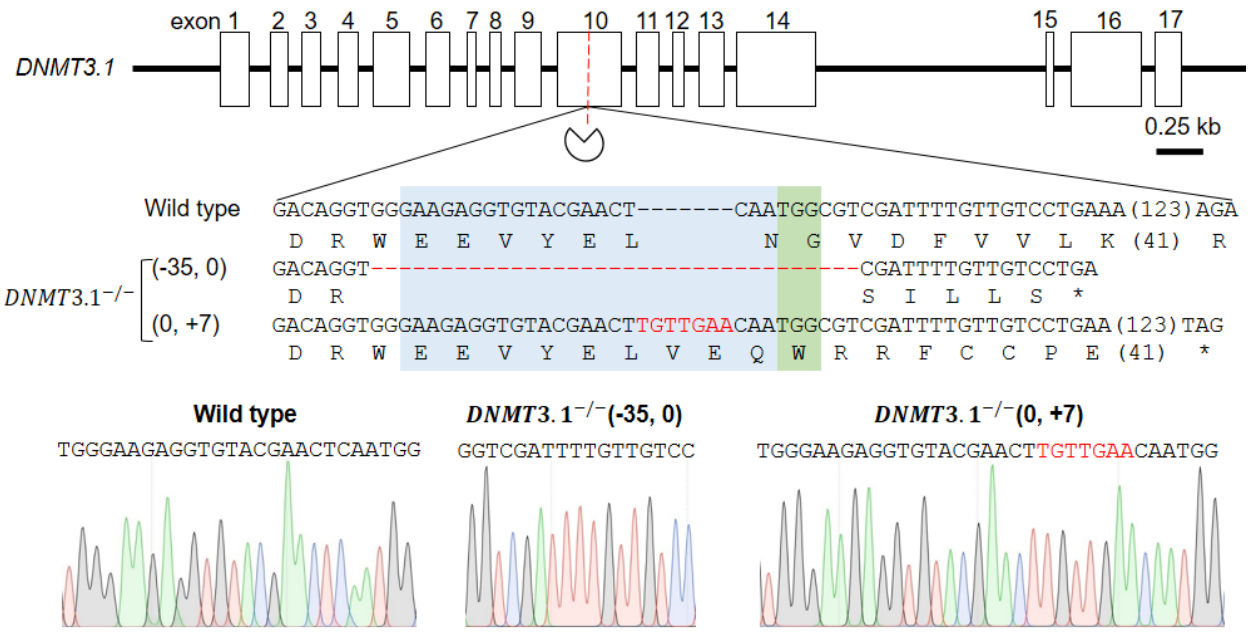

Figure 3.4 CRISPR/Cas-mediated mutagenesis Genomic sequence of the *DapmaDNMT3.1* mutant around the gRNA-targeted site. The DapmaDNMT3.1 (DNMT3.1) exons and introns were illustrated in white boxes and black lines, respectively. In the alignment, the top line represented the wild type *DNMT3.1* nucleotide sequence and deduced amino acid sequence is shown under the DNA sequence. Subsequent lines show sequences of mutant alleles followed by deduced amino acid sequences. The asterisk represents a premature STOP codon. The length (base pairs) of an abbreviated sequence and amino acid sequence are shown in parentheses among the sequences. The length (base pairs) of each indel mutation is written on the left of each sequence (-, deletions; +, insertion). The gRNA recognition and protospacer adjacent motif (PAM) sequences are in blue and green boxes, respectively. Red hyphens and letters indicate the identified mutations. Sanger Sequencing chromatograms of DNA from wild type and the biallelic mutant of *DNMT3.1* were shown below the alignment.

3.3.2 DNMT3.1 mutation does not change growth and fecundity under nutrient-rich conditions.

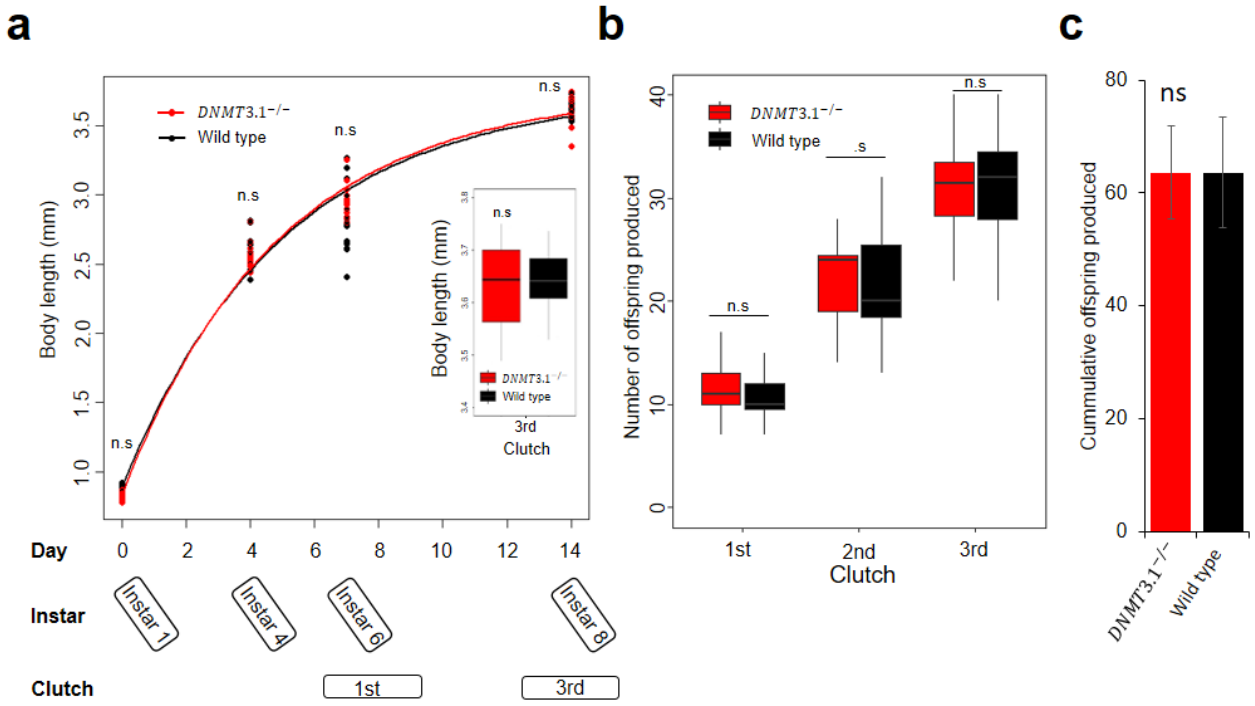

Figure 3.5 Life-history traits of wild type and *DNMT3.1*$^{-/-}$ under nutrient-rich conditions. (**a**) Body length measurements and fitted von Bertalanffy growth for 15 *D. magna* individuals of *DNMT3.1*$^{-/-}$ and wild type. Red and black lines correspond to fitted curved for *DNMT3.1*$^{-/-}$ and wild type, respectively, and boxplot of their body lengths at 3rd clutch stage. (**b**) Boxplot of the 15 *D. magna*'s clutch sizes cultured individually in a nutrient-rich condition. All boxplot whiskers extend to the highest and lowest values, and the boxes extended from quartile 1 to quartile 3, with the middle line showing the median. n.s. denote no significant differences by pairwise *t*-test. (**c**) Bar graph of the cumulative offspring produced from the 15 individuals at 3rd clutch. Error bars indicate the standard deviation of the mean. n.s. denote no significant difference by unpaired *t*-test.

We investigated the phenotypes of the mutant line under nutrient-rich conditions (5.12×10^7 *Chlorella* cells/daphnid). We cultured the wild type and *DNMT3.1*$^{-/-}$ for 14 days and divided this culturing period into two phases, 1) growth phase (0-4 day) and 2) growth and reproduction phase (4-14 day), where growth and reproduction compete for energy from the food. The growth rate

was measured in each phase, and the number of offspring was counted in each clutch. In the growth phase, the growth rate of *DNMT3.1*$^{-/-}$ was similar to that of wild type ($P = 0.14$) (Fig. 3.5 and Table 3.2). In the growth and reproduction phase, there was also no significant difference in the growth rate ($P = 0.2$) in addition to the number of offspring at each clutch or their cumulative clutch size ($P = 0.7$) between wild type and mutant lines (Fig. 3.5b, c and Table 3.2).

Table 3.2. Growth rate and clutch size of *D. magna* under nutrient-rich and starved conditions.

Condition	Age (day)	Instar	Phase	Growth rate (day^{-1})		Clutch		
Nutrient-rich							Wild type	*DNMT3.2*$^{-/-}$
	0-4	1-4	Growth	0.281±0.009	0.283±0.007		nr	nr
	4-14	4-8	Growth + Reproduction	0.033±0.005	0.035±0.004	1st	10.9±2.3	11.4±2.9
						2nd	21.6±5.5	22.3±3.9
						3rd	31.1±5.5	31.9±5.7
Starved	0-4	1-4	Growth	0.263±0.011	0.255±0.02		nr	nr
	4-14	4-8	Growth + Reproduction	0.051±0.01	0.082±0.012***	1st	11.2±1.2	10.3±1.7
						2nd	13.3±1.9	9.2±2.6***
						3rd	8.55±2.7	3.2±1.7***
	14-22	8-10	Reproduction	0.007±0.004	0.008±0.005	4th	4.7±1.5	3.85±1.8
						5th	8.65±2.6	8.35±2.2

Values are mean ± SD; n = 15 in the nutrient-rich and n = 20 in the starved. nr: not related. Significant differences between wild type versus *DNMT3.1*$^{-/-}$, were indicated by asterisks via pairwise t-test, $^{***}P<0.001$.

3.3.3 DNMT3.1 controls the trade-off between growth and fecundity under starved conditions.

We previously found upregulation of DNMT3.1 expression in response to caloric restriction 95. We compared phenotypes between wild type and *DNMT3.1*$^{-/-}$ mutant under starved conditions where the number of *Chlorella* was reduced 8-fold compared to that in nutrient-rich conditions.

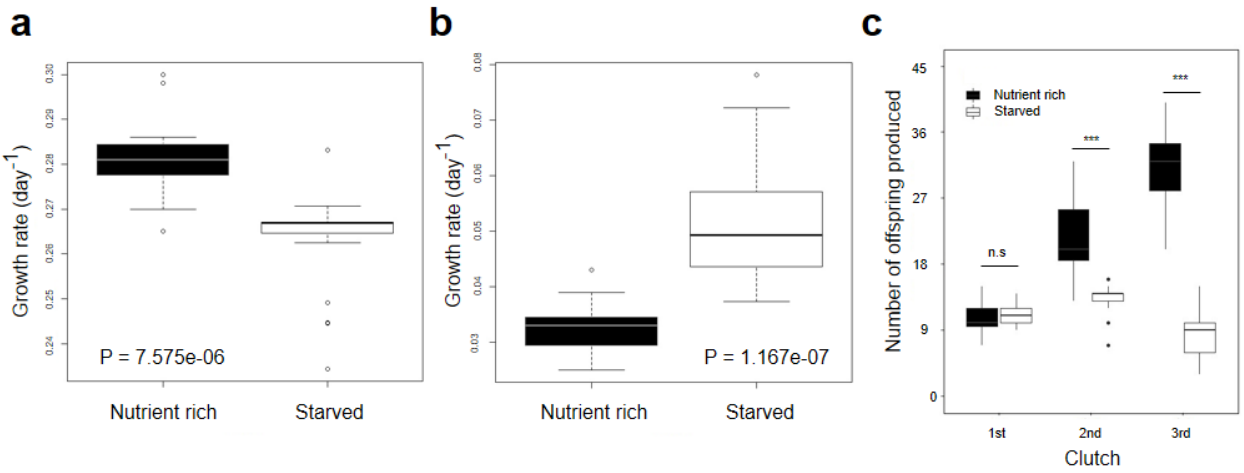

Figure 3.6 Growth rate and clutch size of wild type under nutrient-rich and starved conditions. (**a**) The growth rate of wild types from day 0 to day 4 (growth phase), (**b**) Growth rate of wild types from day 4 to day 14 (growth and reproduction phase). (**a),** (**b**) Boxplot of the growth rate of 15 and 20 wild types cultured individually in nutrient-rich and starved conditions, respectively. All boxplot whiskers extend to the highest and lowest values, and the boxes extended from quartile 1 to quartile 3, with the middle line showing the median. Significance was analyzed using the student's t-test with Welch's correction, P<0.05. (**c**) Boxplot of the clutch sizes of 15 and 20 wild types cultured individually in nutrient-rich and starved conditions. Asterisks denote significant differences by student's t-test with Welch's correction; n.s., not significant; ***$P < 0.001$

We first examined the effects of starvation on growth rate and reproduction in wild-type daphnids. The growth rate was reduced in the growth phase compared to nutrient-rich conditions (P = 7.575e-06) (Fig. 3.6a). In the growth and reproduction phase, starved daphnids' growth rate was higher than that of well-fed daphnids (P = 1.167e-07) (Fig. 3.6b). The starved daphnids produced a smaller number of eggs since the second clutch (Fig. 3.6c). This reduction of the food did not lead to a significant difference in the timing of molting between nutrient-rich and starved conditions.

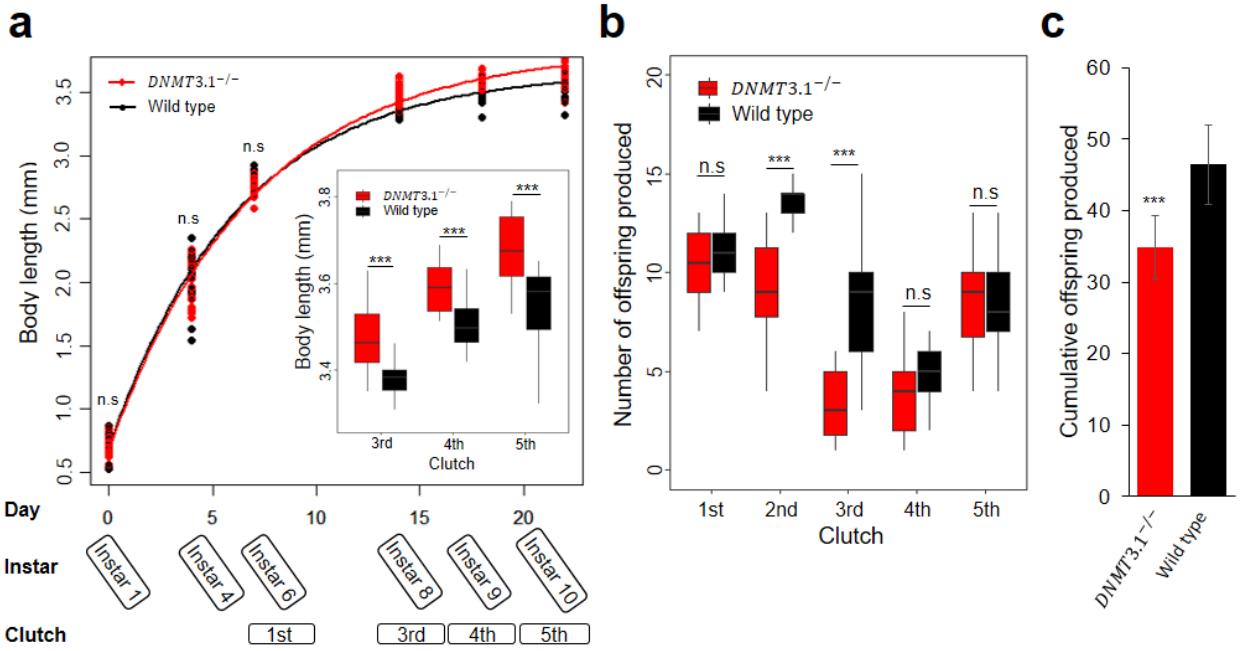

Figure 3.7 Life-history traits of wild type and *DNMT3.1*$^{-/-}$ under starved condition (**a**) Body length measurements and fitted von Bertalanffy growth for 20 *D. magna* individuals of wild type and *DNMT3.1*$^{-/-}$. Red and black lines correspond to fitted curves for *DNMT3.1*$^{-/-}$ and wild type, respectively, and boxplot of their body lengths from 3rd to 5th clutch stages. (**b**) Boxplot of the 20 *D. magna*'s clutch sizes cultured individually in starved condition. All boxplot whiskers extend to the highest and lowest values, and the boxes extended from quartile 1 to quartile 3, with the middle line showing the median. Asterisks denote significant differences by pairwise *t*-test; n.s., not significant; ***P < 0.001. (**c**) Bar graph of the cumulative offspring produced from the 20 individuals at 5th clutch. Error bars indicate the standard deviation of the mean. Asterisks denote significant differences by unpaired *t*-test; ***P < 0.001.

We next investigated phenotypes of *DNMT3.1*$^{-/-}$ mutants. There was no difference in growth (P = 0.12) between the wild type and the mutant in the growth phase (Fig. 3.7 and Table 1). However, in the growth and reproduction phase, the growth rate of mutant daphnids (0.082 mm/day) was higher than that of wild type (0.051 mm/day) (P = 2.5E-10) (Fig. 3.7a and Table 3.2). In contrast, mutants produced a smaller number of offspring at the second and third clutches compared to the wild type (P = 1.6E-06 and 8.7E-09, respectively) (Fig. 3.7b and Table 3.2). This

phase's phenotypic differences motivated us to extend observation until 22 days-old for investigations of the phenotypes. We named this third period the reproduction phase because the growth rate in this phase becomes much lower than that in the earlier two phases. In the reproduction phase, we observed no differences in growth rate and clutch size between wild types and mutants (Fig. 3.7 and Table 3.2). The timing of molting did not differ between wild type and *DNMT3.1*$^{-/-}$ mutants.

3.3.4 DNMT3.1 mutation reduces life span under starved conditions.

We compared the life span of the DNMT3.1 mutant to that of the wild-type. In the nutrient-rich condition, wild type and *DNMT3.1*$^{-/-}$ lines showed similar longevity (log-rank $p = 0.9$), with a median lifespan of 54 and 56 days, respectively (Fig. 3.8). In the starved condition, a decreased trend in the lifespan of the *DNMT3.1*$^{-/-}$ line was observed (log-rank $p = 0.0136$) with a median lifespan of 50 days compared to 61 days of the wild type line (Fig. 3.8).

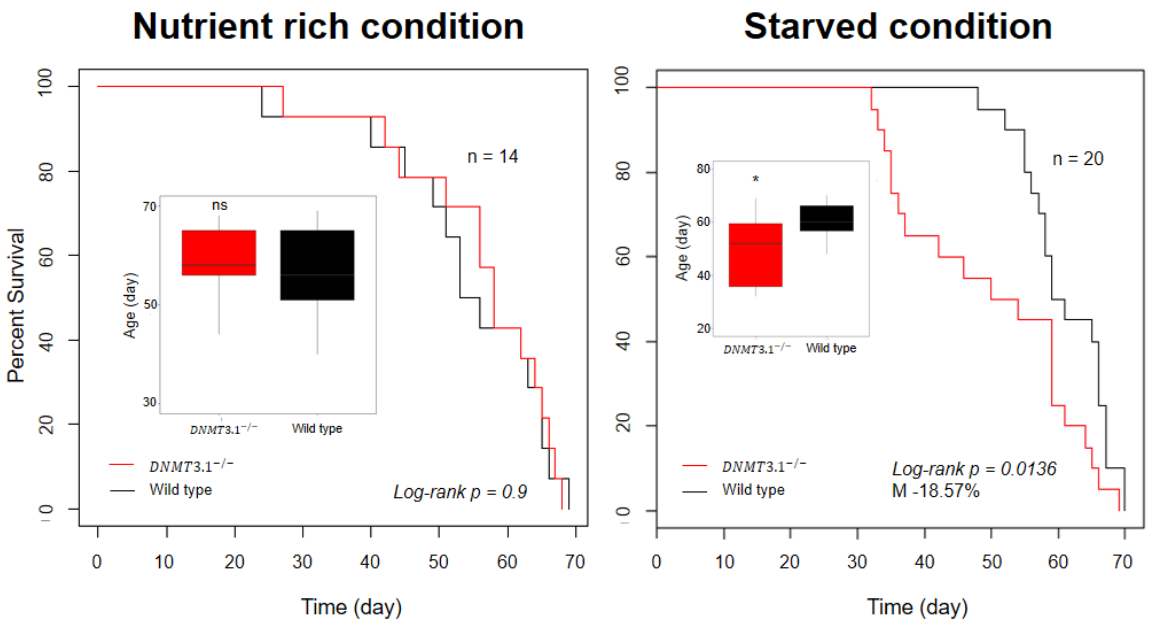

Figure 3.8 Life-span of wild type and *DNMT3.1*$^{-/-}$ under nutrient-rich and starved conditions. Kaplan-Meier survival curves of wild type and *DNMT3.1*$^{-/-}$, and boxplot of their ages. M indicates a decrease in the median lifespan of *DNMT3.1*$^{-/-}$. The *p*-value was determined using the log-rank test. Asterisk denotes significant differences by pairwise *t*-test; n.s., not significant; *$P < 0.05$

3.3.5 DNMT3.1 mutation alters transcriptome under starved conditions.

We examined whether the other DNMT genes compensate for the DNMT3.1 mutation in this phase or not. RT-qPCR compared the expression of DNMT1, DNMT3.1, and DNMT3.2 between wild type and *DNMT3.1*$^{-/-}$ either under nutrient-rich or starved conditions. The result showed no interaction between DNMT3.1 and any other two DNMT genes (Table 3.3). Upregulation of *DNMT3.1* expression in response to the starved condition was also confirmed both in wild type and *DNMT3.1*$^{-/-}$ (Figure 3.9).

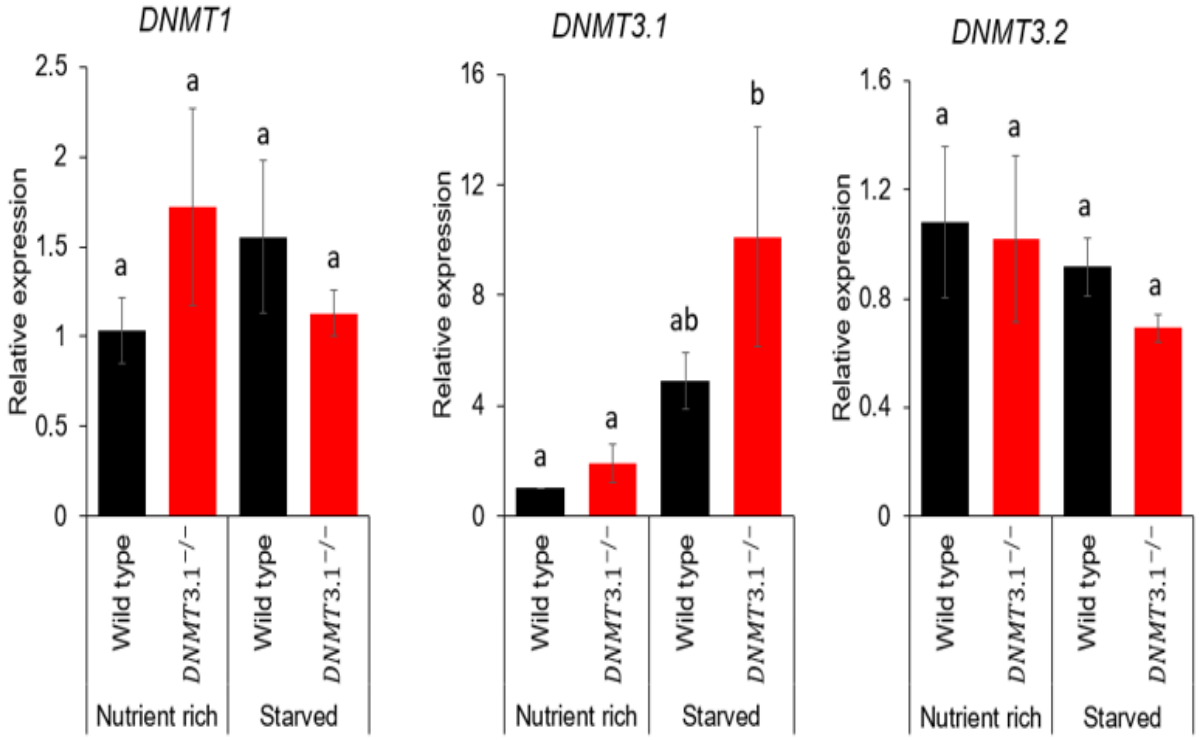

Figure 3.9 Relative expression of *DapmaDNMTs* in wild type and mutant under nutrient-rich and starved conditions. Relative expression of *DapmaDNMTs* in 12 days adults cultured in nutrient-rich and starved conditions. Data were expressed as the mean fold change of starved wild type, nutrient-rich and starved mutants with nutrient-rich wild type as the calibrator. Normalization was performed using *Ribosomal protein L32* gene expression as the internal control. Error bars indicate the standard error of the mean (n = 3). Treatment with the different letter are significantly different ($P < 0.05$) identified by Fisher's LSD test in multiple comparisons after two-way ANOVA.

Table 3.3. Summary of two-way ANOVA for food level and line on the expression of *DNMT* genes.

Gene	Source of variation	Df	SS	MS	*F*	*P*
DNMT1	FOOD (F)	1	0.0037	0.00367	0.0092	0.9261
	LINE (L)	1	0.0547	0.05467	0.1363	0.7216
	Interaction F × L	1	0.9241	0.92408	2.3031	0.1676
DNMT3.1	FOOD (F)	1	109.324	109.324	8.3404	**0.0202**
	LINE (L)	1	28.275	28.275	2.1571	0.1801
	Interaction F × L	1	13.954	13.954	1.0645	0.3323
DNMT3.2	FOOD (F)	1	0.18253	0.182533	1.3241	0.2831
	LINE (L)	1	0.06163	0.061633	0.4471	0.5225
	Interaction F × L	1	0.0192	0.0192	0.1393	0.7187

Df, Degrees of freedom; SS, Single squares; MS, Mean squares. Significant effect is highlighted in bold ($P \leq 0.05$)

To examine how many genes were affected at mRNA level in the DNMT3.1 mutation, we performed RNA-Seq analysis to find differentially expressed genes (DEGs) between wild-type and mutant lines in the second phase, growth and reproduction phase.

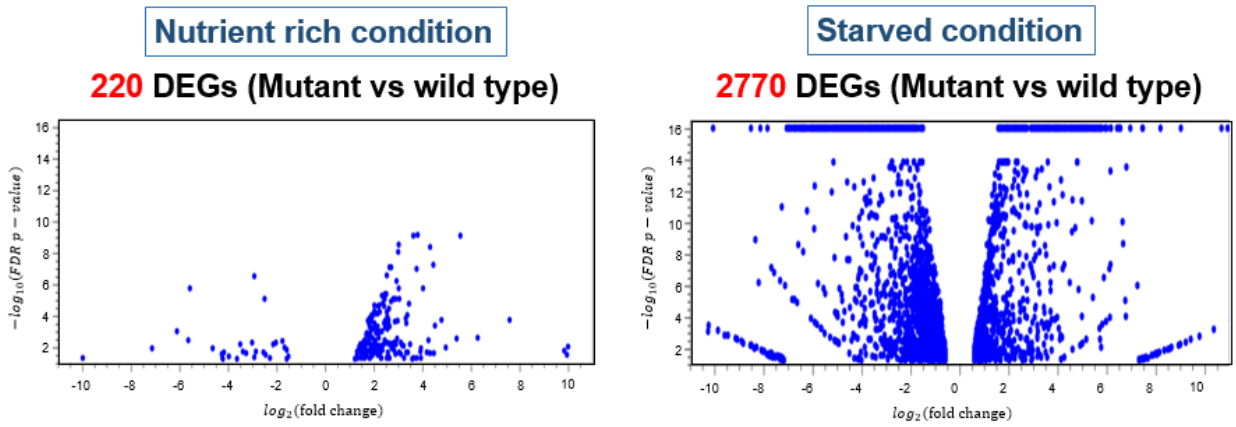

Figure 3.10 Volcano plot of RNA-seq transcriptome data displaying the pattern of gene expression values for mutant relative to wild type cultured under nutrient-rich and starved conditions. Each dot represents one differential expression gene (DEG) (FDR *p*-value ≤ 0.05 and Fold change ≥ $|1.5|$)

In nutrient-rich and starved conditions, numbers of differentially expressed genes were 220 and 2770 respectively (Fig. 3.10), demonstrating that, in the starved condition, disruption of DNMT3.1 showed a much larger effect on the transcriptomes.

Amongst the DEGs in starved animals, 1432 annotated genes were identified, and we performed clustering of these by k-Means. 1364 genes passed the filter (as described in Materials and Methods) and were divided into five clusters (Fig. 3.11). Furthermore, we analyzed the gene ontology (GO) for functional annotation of genes in each cluster by using Fisher's Exact Test (accession number: GSE158129). Clusters A and B included genes showing higher expression in the mutant under starved conditions. The top enriched GOs in clusters A and B were mitotic cell cycle and transmembrane transport, respectively (Table 2). In cluster A, we found a notable gene, *Nuclear hormone receptor ftz-f1 (Dapma7bEVm011018t1) (ftz-f1),* that showed an upregulation in the mutant under starved conditions (Table 3.4). Interestingly, in cluster B, we found a gene that codes for an ortholog of *solute carrier family 13 member 5* (*Dapma7bEVm010715t1*), known as *Slc13a5* or *INDY* (*I'm not dead yet*). The *Daphnia INDY* ortholog showed reduced expression in the wild type but upregulated expression in the mutant under starvation (Table 3.4 and accession number: GSE158129). Genes in Cluster C showed down-regulation in both wild type and mutant under the starved condition and were more severely down-regulated in the mutant (Fig. 3.11). Importantly, *vitellogenin* genes, *vtg1* (*Dapma7bEVm024402t1*), and seven other genes related to lipid transport were included in this cluster (accession number: GSE158129). Cluster D represented down-regulated genes in the mutant under starved conditions, many of which are involved in carbohydrate metabolic processes (Fig. 3.11 and Table 3.4). We found a represented gene, *target of brain insulin (Dapma7bEVm003111t1)* known as *tobi*, an α-glucosidase. Finally, cluster E genes were upregulated in the wild type under starved conditions, which included genes

related to protein turnover (proteolysis) (Fig. 3.11 and Table 3.4). A represented gene of this GO was *trypsin (Dapma7bEVm010425t1),* known as *epsilonTry*.

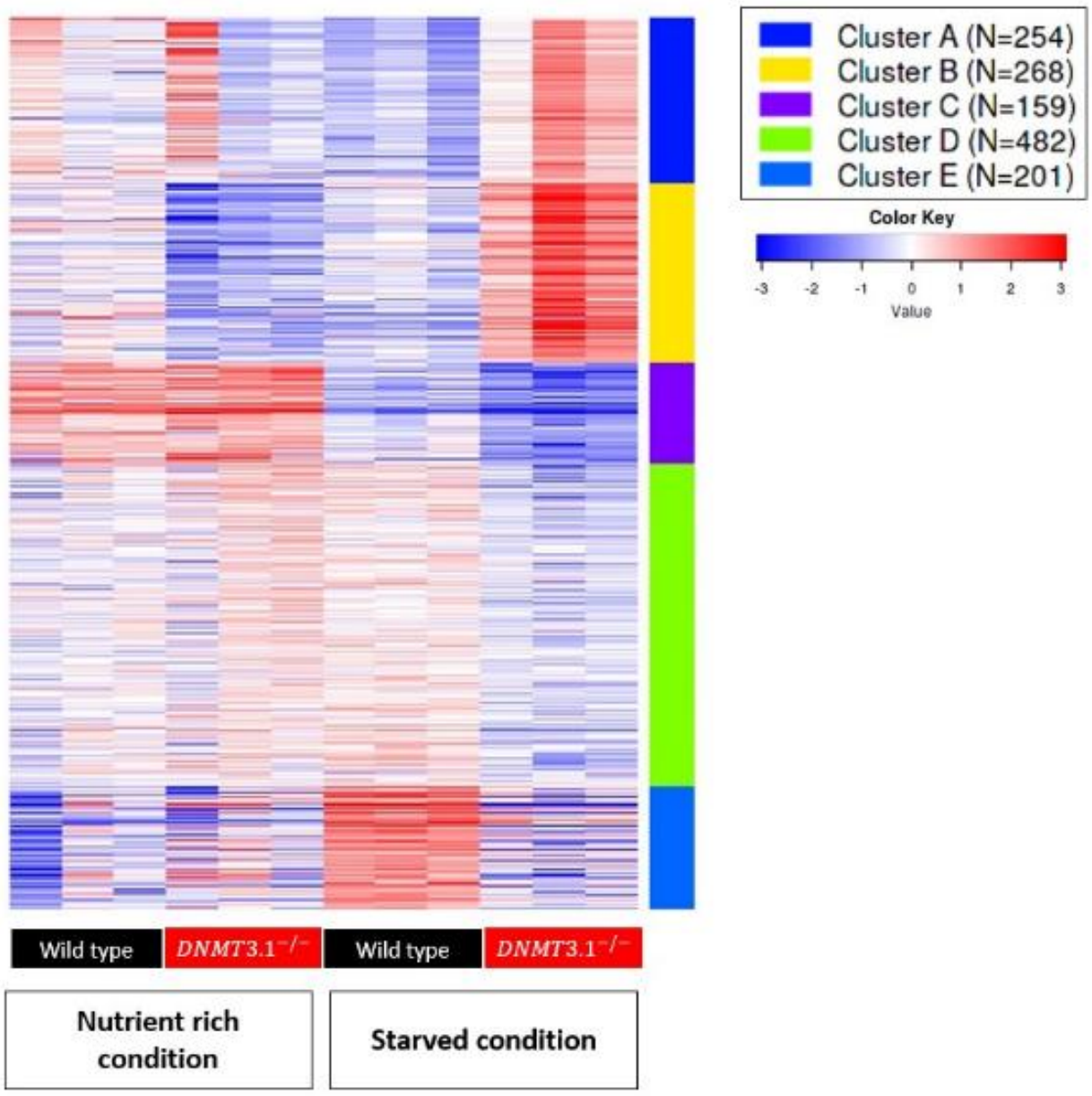

Figure 3.11 K-means clustering of DEGs from wild type and *DNMT3.1*$^{-/-}$ in two conditions. Heatmap generated based on clustering 1364 annotated differential expression genes in the dataset into 5 clusters.

Table 3.4. Top gene ontology category in each cluster, and notable genes found in the cluster.

Cluster	Gene Ontology (GO) Term Enrichment		Notable Genes	Differential Expression (MTvsWT)	
	Top GO Biological Process Category	FDR *P*-value		FC	FDR *P*-value
A	Mitotic cell cycle	9.94E-17	*Ftz-f1 (Dapma7bEVm011018t1)*	2.53	4.28E-10
B	Transmembrane transport	3.83E-07	*INDY (Dapma7bEVm010715t1)*	41.17	0
C	Proteolysis	1.79E-13	*Vtg1 (Dapma7bEVm024402t1)*	-2.45	6.74-E-09
D	Carbohydrate metabolic process	6.39E-17	*tobi (Dapma7bEVm003111t1)*	-2.26	1.24E-05
E	Proteolysis	2.38E-09	*epsilonTry (Dapma7bEVm010425t1)*	-3.22	4.22E-06

MT: *DNMT3.1*$^{-/-}$ mutant; WT: Wild type; FDR: False discovery rate; FC: Fold change expression between mutant and wild type under starved conditions.

3.3 Discussion

Despite the long history of research on energy allocation, genes affecting energy allocation still remain mostly unknown. In the cladoceran crustacean *D. magna*, energy allocation among competing life-history traits have been extensively investigated under starved conditions. We have previously shown that *Daphnia DNMT3.1* was up-regulated in response to starvation, suggesting a potential function of this gene for energy allocation. This study introduced a mutation into *DNMT3.1* and analyzed phenotypes of its mutant under caloric restriction. The resulting biallelic mutant is viable and did not show any change in growth rate, reproduction, and longevity under nutrient-rich conditions.

In contrast, under starved conditions, the growth rate of this DNMT3.1 mutant was increased. However, its reproduction was reciprocally reduced compared to the wild type when the growth and reproduction activities competed during a period from instar 4 to 8. The life span of this mutant was significantly shorter than that of the wild type. We also compared transcriptomes between DNMT3.1 mutant and wild type under nutrient-rich and starved conditions. Consistent with the DNMT3.1 mutant phenotypes, the starved condition led to changes in the

mutant transcriptomes, including differential expression of vitellogenin genes. In addition, we found upregulation of the *I am not dead yet* (*INDY*) ortholog, which has been known to shorten the life span in *Drosophila*, explaining the shorter life span of the DNMT3.1 mutant. These results establish DNMT3.1 as a critical regulator for life span and energy allocation between growth and reproduction during caloric restriction. Our findings reveal how energy allocation is implemented by selective expression of a DNMT3 ortholog that is widely distributed among animals. We also infer a previously unidentified *Daphnia* adaptation that invests more energy for reproduction than growth under starved conditions.

3.3.1 DNMT3.1 controls the trade-off between growth and reproduction under starved conditions.

The trade-off between growth and reproduction occurred in both wild-type and DNMT3.1 mutants under different food levels, which is in line with previous reports [27]. Interestingly, the DNMT3.1 mutant showed a higher growth rate and lower clutch size compared to wild type when both processes competed during a period from instar 4 to 8, indicating that DNMT3.1 allocates more energy to reproduction. These results suggest that DNMT3.1 controls the trade-off between growth and reproduction when growth and fecundity compete for energy from the food. Larger clutch size has a positive impact on expanding its population size, which in turn would lead to an increase in fitness. The correlation of DNMT3.1 gene activity with phenotypes in the natural population needs to be examined to further understand the functions of this gene in an ecological context.

3.3.2 DNMT3.1 increases life span under starved conditions.

The life span of the wild type was longer than that of DNMT3.1 mutant under starved conditions. In *D. melanogaster*, starvation reduced *I am not dead yet,* or *INDY* expression and in

turn led to extension for longevity[109 110]. INDY functions as a citrate transporter of the Krebs cycle and modulates energy production during the life span [111]. Interestingly, in *D. magna*, we found upregulation of *INDY* in short-lived DNMT3.1 mutants under starved conditions. Thus, we hypothesize that, in the wild type, DNMT3.1 downregulates *INDY* and extends its life span under starved conditions. To test this hypothesis, functional analysis of the *Daphnia INDY* ortholog would be needed in the future.

3.3.3 Possible physiological function of DNMT3 ortholog in pancrustaceans.

DNMT3 orthologs are phylogenetically distributed even in invertebrates, but their functions still remain unclear because invertebrate models such as *Caenorhabditis elegans* and *D. melanogaster* lack the DNMT3 ortholog and DNA methylation on the genome. In *D. magna*, DNMT3.1 mutant is viable and did not show any developmental changes under nutrient-rich conditions. Consistent with this phenotype, knockdown of DNMT3 orthologs in social insects did not reduce survivability [21,92,93]. Although we need to confirm how much the DNMT3.1 protein level has been reduced in the DNMT3.1 mutant, the DNMT3 ortholog may not function in basal in arthropods development, unlike mammalian DNMT3. In flies, InR and FOXO are known to control life span and fecundity [33–35]. Since a potential FOXO binding site has been found in a promoter region of DNMT3.1, core components like the FOXO signaling pathway that influence life history traits may be conserved and linked to DNMT3.1 as a downstream component. Functional analyses of DNMT3 orthologs in other pancrustaceans under stressed conditions, including starvation, will lead to a better understanding of this gene's functions in the control of life-history traits.

3.3.4 Possible molecular function of DNMT3.1.

Table 4.1 Gene expression of hypermethylated genes from wild type (WT) and mutant (MT) in a starved condition

Gene ID	Gene name	DMR	WT	MT
Dapma7bEVm004172t1	SHC SH2 domain-binding protein	Hypermethylated	Down	No
Dapma7bEVm010768t1	Surfeit locus protein	Hypermethylated	Down	No
Dapma7bEVm003001t1	Structural maintenance of chromosome 2 1 protein	Hypermethylated	Down	No
Dapma7bEVm005181t1	conserved protein	Hypermethylated	Down	No
Dapma7bEVm004398t1	Upstream stimulatory factor	Hypermethylated	Down	No
Dapma7bEVm000396t1	Peroxisomal targeting signal 1 receptor	Hypermethylated	Down	No
Dapma7bEVm002983t1	GTP-binding nuclear protein Ran	Hypermethylated	Down	No
Dapma7bEVm001440t1	Eukaryotic peptide chain release factor gtp-binding subunit erf2 translation release factor 3 erf3 erf-3	Hypermethylated	Down	No

DMR: Differential methylated region was reported [65], No: no change; Down: Down-regulated; Up: Up-regulated

Previously, a study in *Daphnia* has shown 115 genes with significantly hypermethylated regions under starved conditions in *D. magna* [65]. Under the starved condition, of the 115, only 8 showed reduced expression in wild type but were de-repressed upon DNMT3.1 mutation (Table 4.1).

This result may suggest that DNMT3.1 does not have an important role in DNA methylation under starved conditions. Because DNMT3.1 mutation changed life-history traits and expression patterns of 2770 genes under starved conditions, it might regulate gene expression globally, although we could not exclude the possibility that DNMT3.1 controls master regulatory factors involved in starvation responses. In mice, both DNMT3A and DNMT3B function as a transcriptional repressor without catalytic activity in cultured cells [47] In addition, catalytically inactive DNMT3B has been demonstrated to rescue the lethal embryonic phenotype of DNMT3B knockout mice [112], suggesting that DNMT3B has a function independent of DNA methylation.

Taken together, the DNMT3.1 mutant lacking a typical MTase domain and activity has lost control of a large number of genes differentially expressed under the starved conditions.

Among the potential DNMT3.1 target genes under starved conditions, we listed five notable genes, including *INDY* (Table 3.4). *ftz-f1*, a competence factor for juvenile hormone (JH) activation, has essential roles in developmental regulation and various aspects of insect adult life [113,114]. *Vtg1* encodes vitellogenin, a precursor of a major yolk protein [115], and has been used as an indicator of fecundity [94,116]. The downregulation of *Vtg* genes was consistent with the severe decrease of fecundity in mutants in response to the starved condition. *Trypsin* encodes digestive protease in the gut of *D. magna* [117] and has been listed as involved in starvation resistance gene in flies [118].

I demonstrated the physiological function of DNMT3.1 in extending longevity and energy allocation to reproduction under starved conditions. Although DNMT3.1 lacks an evolutionarily conserved sequence of the MTase domain, it changes the global transcriptome in response to starvation.

Chapter 4

General discussions

The utility of *Daphnia magna* for studying on a genetic basis inform us about the molecular mechanisms of energy allocation. In this study, I found that the existence and upregulation of *DNMT3.1* play an important role in regulating the proportional energy allocation between growth and reproduction under food limitations. The loss of DNMT3.1 gene led the organisms to enhance their energy investment to growth and reduced reproduction. Moreover, it clearly showed when the organism was in starved conditions. Therefore, *DNMT3.1* controls the trade-off between growth and reproduction under starved conditions. In addition, due to the fact of annually coping with starvation, *DNMT3.1* also shows its essential role in evolutionary adaption, which helps *D.magna* maintain the population persistence and survive.

Starvation is a well-known factor in resisting insulin when the insulin level has declined [119]. DNMT3.1 upregulated and possibly regulated by FOXO, a Forkhead transcription factor under starved conditions when we found the consensus FOXO binding site sequence in the gene promoter region. This possible regulation of FOXO may be correlated insulin signaling pathway, while under starvation, FOXO is activated to deal with insulin resistance [120]. The targeted disruption of the DNMT3 ortholog in *D. magna* revealed DNMT3.1 controls the trade-off between growth and reproduction by changing the global transcriptomes under starvations. Although DNMT3.1 lacks the conserved methyltransferase motifs, there might be two possibilities. The first possibility is a methylated function.

In comparison to the domain structure of DNMT3s in mammals, DNMT3L lacks methyltransferase motifs as well as could not methylate DNA directly. However, it has been

investigated that DNMT3L facilitates DNMT3A protein to increase methylated level by forming heterotetramers complex, enabling it to bind to nucleosomes, which results in stabilization of DNMT3A protein[18]. The second possibility is as a transcriptional repressor. According to a current study, catalytically inactive DNMT3B restores a majority of molecular changes observed in *DNMT3B*$^{-/-}$ mice [112]. It has been clarified that DNMT3B is a multifaceted protein that is an accessory factor for other DNMT similar to DNMT3L and, as a transcriptional repressor, repress gene expression directly [112].

For future study, the gene regulatory mechanisms of DNMT3.1 can be investigated by investigating DNA methylation and chromatin immunoprecipitation for the identification of direct targets of this protein.

I anticipate that this work will understand the molecular mechanisms underlying energy allocation in the ecologically important *Daphnia* species.

List of publications

Nguyen, N. D., Matsuura, T., Kato, Y. & Watanabe, H. Caloric restriction upregulates the expression of DNMT3.1, lacking the conserved catalytic domain, in *Daphnia magna*. *genesis* e23396 (2020).

Nguyen, N. D., Matsuura, T., Kato, Y. & Watanabe, H. DNMT3.1 controls trade-offs between growth, reproduction, and life span under starved conditions in *Daphnia magna. Sci. rep.* (2021)

References

1. Stearns, S. C. *The Evolution of Life Histories*. *Oxford University Press* (1992).

2. Cox, R. M. *et al.* Experimental evidence for physiological costs underlying the trade-off between reproduction and survival. *Funct. Ecol.* **24**, 1262–1269 (2010).

3. Rapkin, J., Jensen, K., House, C. M., Wilson, A. J. & Hunt, J. Genotype-by-sex-by-diet interactions for nutritional preference, dietary consumption, and lipid deposition in a field cricket. *Heredity (Edinb).* **121**, 361–373 (2018).

4. Cotter, S. C., Littlefair, J. E., Grantham, P. J. & Kilner, R. M. A direct physiological trade-off between personal and social immunity. *J. Anim. Ecol.* **82**, 846–853 (2013).

5. López-Lluch, G. *et al.* Calorie restriction induces mitochondrial biogenesis and bioenergetic efficiency. *Proc. Natl. Acad. Sci. U. S. A.* **103**, 1768 LP – 1773 (2006).

6. Mattson, M. P. & Wan, R. Beneficial effects of intermittent fasting and caloric restriction on the cardiovascular and cerebrovascular systems. *J. Nutr. Biochem.* **16**, 129–137 (2005).

7. Kumar, S. *et al.* The DNA (cytosine-5) methyltransferases. *Nucleic Acids Res.* **22**, 1–10 (1994).

8. Hass, B. S., Hart, R. W., Lu, M. H. & Lyn-Cook, B. D. Effects of caloric restriction in animals on cellular function, oncogene expression, and DNA methylation in vitro. *Mutat. Res.* **295**, 281–289 (1993).

9. Kim, C. H. *et al.* Short-term calorie restriction ameliorates genomewide, age-related alterations in DNA methylation. *Aging Cell* **15**, 1074–1081 (2016).

10. Schaefer, M. & Lyko, F. DNA methylation with a sting: An active DNA methylation

system in the honeybee. *BioEssays* **29**, 208–211 (2007).

11. Bird, a P. CpG-rich islands and the function of DNA methylation. *Nature* **321**, 209–213 (1986).

12. Lyko, F. The DNA methyltransferase family: A versatile toolkit for epigenetic regulation. *Nat. Rev. Genet.* **19**, 81–92 (2018).

13. Goll, M. G. & Bestor, T. H. Eukaryotic Cytosine Methyltransferases. *Annu. Rev. Biochem.* **74**, 481–514 (2005).

14. Chen, T. *et al.* Complete inactivation of DNMT1 leads to mitotic catastrophe in human cancer cells. *Nat. Genet.* **39**, 391–396 (2007).

15. Okano, M., Bell, D. W., Haber, D. A. & Li, E. DNA methyltransferases Dnmt3a and Dnmt3b are essential for de novo methylation and mammalian development. *Cell* **99**, 247–257 (1999).

16. Li, E., Beard, C. & Rudolf, B. Role for DNA methylation in genomic imprinting. *Nature* **366**, 362–366 (1993).

17. Hata, K., Okano, M., Lei, H. & Li, E. Dnmt3L cooperates with the Dnmt3 family of de novo DNA methyltransferases to establish maternal imprints in mice. *Development* **129**, 1983–1993 (2002).

18. Jia, D., Jurkowska, R. Z., Zhang, X., Jeltsch, A. & Cheng, X. Structure of Dnmt3a bound to Dnmt3L suggests a model for de novo DNA methylation. *Nature* **449**, 248–251 (2007).

19. Wang, Y. *et al.* Functional CpG methylation system in a social insect. *Science.* **314**, 645–647 (2006).

20. Lyko, F. & Maleszka, R. Insects as innovative models for functional studies of DNA methylation. *Trends Genet.* **27**, 127–131 (2011).

21. Kucharski, R., Maleszka, J., Foret, S. & Maleszka, R. Nutritional control of reproductive status in honeybees via DNA methylation. *Science.* **319**, 1827–1830 (2008).

22. Biergans, S. D., Giovanni Galizia, C., Reinhard, J. & Claudianos, C. Dnmts and Tet target memory-associated genes after appetitive olfactory training in honey bees. *Sci. Rep.* **5**, 16223 (2015).

23. Li-Byarlay, H. *et al.* RNA interference knockdown of DNA methyl-transferase 3 affects gene alternative splicing in the honey bee. *Proc. Natl. Acad. Sci.* **110**, 12750–12755 (2013).

24. Kooijman, S. A. L. M. Population Dynamics on Basis of Budgets. in *The Dynamics of Physiologically Structured Populations* (eds. Metz, J. A. J. & Diekmann, O.) 266–297 (Springer-Verlag Berlin Heidelberg, 1986). doi:10.1007/978-3-662-13159-6

25. Mccauley, E. *et al.* The Physiological Ecology of *Daphni*a : Development of a Model of Growth and Reproduction. *Ecology* **71**, 703–715 (1990).

26. Bradley, M. C., Perrin, N. & Calow, P. Energy allocation in the cladoceran *Daphnia magna* Straus , under starvation and refeeding. *Oecologia* **86**, 414–418 (1991).

27. Glazier, D. S. & Calow, P. Energy allocation rules in *Daphnia magna*: clonal and age differences in the effects of food limitation. *Oecologia* **90**, 540–549 (1992).

28. Sommer, U. *et al.* Beyond the Plankton Ecology Group (PEG) Model: Mechanisms Driving Plankton Succession. *Annu. Rev. Ecol. Evol. Syst.* **43**, 429–448 (2012).

29. Orsini, L. *et al.* Data Descriptor : *Daphnia magna* transcriptome by RNA-Seq across 12 environmental stressors. *Sci. Data* **3**, 1–16 (2016).

30. Lee, B.-Y. *et al.* The genome of the freshwater water flea Daphnia magna: A potential use for freshwater molecular ecotoxicology. *Aquat. Toxicol.* **210**, 69–84 (2019).

31. Nakanishi, T., Kato, Y., Matsuura, T. & Watanabe, H. CRISPR/Cas-mediated targeted mutagenesis in Daphnia magna. *PLoS One* **9**, (2014).

32. Kumagai, H., Nakanishi, T., Matsuura, T., Kato, Y. & Watanabe, H. CRISPR/Cas-mediated knock-in via nonhomologous end-joining in the crustacean *Daphnia magna*. *PLoS One* **12**, 1–12 (2017).

33. Paaby, A. B., Blacket, M. J., Hoffmann, A. A. & Schmidt, P. S. Identification of a candidate adaptive polymorphism for *Drosophila* life history by parallel independent clines on two continents. *Mol. Ecol.* **19**, 760–774 (2010).

34. Paaby, A. B., Bergland, A. O., Behrman, E. L. & Schmidt, P. S. A highly pleiotropic amino acid polymorphism in the *Drosophila* insulin receptor contributes to life-history adaptation. *Evolution (N. Y).* **68**, 3395–3409 (2014).

35. Durmaz, E. *et al.* A clinal polymorphism in the insulin signaling transcription factor foxo contributes to life-history adaptation in *Drosophila*. *Evolution (N. Y).* **73**, 1774–1792 (2019).

36. Zhu, C. T., Chang, C., Reenan, R. A. & Helfand, S. L. Indy gene variation in natural populations confers fitness advantage and life span extension through transposon insertion. *Aging (Albany. NY).* **6**, 58–69 (2014).

37. Law, J. A. & Jacobsen, S. E. Establishing, maintaining and modifying DNA methylation patterns in plants and animals. *Nat. Rev. Genet.* **11**, 204–220 (2010).

38. Feil, R. & Fraga, M. F. Epigenetics and the environment: Emerging patterns and implications. *Nat. Rev. Genet.* **13**, 97–109 (2012).

39. Lande-Diner, L. & Cedar, H. Silence of the genes - Mechanisms of long-term repression. *Nat. Rev. Genet.* **6**, 648–654 (2005).

40. Reik, W. & Lewis, A. Co-evolution of X-chromosome inactivation and imprinting in mammals. *Nat. Rev. Genet.* **6**, 403–410 (2005).

41. Reik, W. & Walter, J. Genomic imprinting: parental influence on the genome. *Nat. Rev. Genet.* **2**, 21–32 (2001).

42. Monk, M., Boubelik, M. & Lehnert, S. Temporal and regional changes in DNA methylation in the embryonic, extraembryonic and germ cell lineages during mouse embryo development. *Development* **99**, 371–382 (1987).

43. Waterland, R. A. & Jirtle, R. L. Transposable Elements: Targets for Early Nutritional Effects on Epigenetic Gene Regulation. *Mol. Cell. Biol.* **23**, 5293–5300 (2003).

44. Ruiz-Hernandez, A. *et al.* Environmental chemicals and DNA methylation in adults: a systematic review of the epidemiologic evidence. *Clin. Epigenetics* **7**, 55 (2015).

45. Alvarado, S., Rajakumar, R., Abouheif, E. & Szyf, M. Epigenetic variation in the Egfr gene generates quantitative variation in a complex trait in ants. *Nat. Commun.* **6**, 6513 (2015).

46. Okano, M., Xie, S. & Li, E. Cloning and characterization of a family of novel mammalian

DNA (cytosine-5) methyltransferases. *Nat. Genet.* **19**, 219–220 (1998).

47. Bachman, K. E., Rountree, M. R. & Baylin, S. B. Dnmt3a and Dnmt3b Are Transcriptional Repressors That Exhibit Unique Localization Properties to Heterochromatin. *J. Biol. Chem.* **276**, 32282–32287 (2001).

48. Chédin, F. *The DNMT3 family of mammalian de novo DNA methyltransferases*. *Progress in Molecular Biology and Translational Science* **101**, (2011).

49. Qiu, C., Sawada, K., Zhang, X. & Cheng, X. The PWWP domain of mammalian DNA methyltransferase Dnmt3b defines a new family of DNA-binding folds. *Nat. Struct. Biol.* **9**, 217–224 (2002).

50. Dhayalan, A. *et al.* The Dnmt3a PWWP domain reads histone 3 lysine 36 trimethylation and guides DNA methylation. *J. Biol. Chem.* **285**, 26114–26120 (2010).

51. Otani, J. *et al.* Structural basis for recognition of H3K4 methylation status by the DNA methyltransferase 3A ATRX-DNMT3-DNMT3L domain. *EMBO Rep.* **10**, 1235–1241 (2009).

52. Zhang, Y. *et al.* Chromatin methylation activity of Dnmt3a and Dnmt3a/3L is guided by interaction of the ADD domain with the histone H3 tail. *Nucleic Acids Res.* **38**, 4246–4253 (2010).

53. Cheng, X. Structure and Function of DNA Methyltransferases. *Annu. Rev. Biophys. Biomol. Struct.* **24**, 293–318 (1995).

54. Li, B. *et al.* DNA methyltransferase BmDnmt1 and BmDnmt2 in silkworm (*Bombyx mori*) and the regulation of silkworm embryonic development. *Arch. Insect Biochem. Physiol.*

100, 1–12 (2019).

55. Hebert, P. D. & Ward, R. D. Inheritance during parthenogenesis in *Daphnia magna*. *Genetics* **71**, 639–642 (1972).

56. Hebert, P. D. N. The Population Biology of *Daphnia* (Crustacea, Daphnidae). *Biol. Rev.* **53**, 387–426 (1978).

57. Laforsch, C., Ngwa, W., Grill, W. & Tollrian, R. An acoustic microscopy technique reveals hidden morphological defenses in *Daphnia*. *Proc. Natl. Acad. Sci. U. S. A.* **101**, 15911–15914 (2004).

58. Hood, J. M. & Sterner, R. W. Carbon and phosphorus linkages in *Daphnia* growth are determined by growth rate, not species or diet. *Funct. Ecol.* 1156–1165 (2014). doi:10.1111/1365-2435.12243

59. Harris, K. D. M., Bartlett, N. J. & Lloyd, V. K. *Daphnia* as an emerging epigenetic model organism. *Genet. Res. Int.* **2012**, 147892 (2012).

60. Vandegehuchte, M. B. *et al.* Occurrence of DNA methylation in *Daphnia magna* and influence of multigeneration Cd exposure. *Environ. Int.* **35**, 700–706 (2009).

61. Strepetkait, D. *et al.* Analysis of DNA methylation and hydroxymethylation in the genome of crustacean *Daphnia pulex*. *Genes (Basel).* **7**, 1–14 (2015).

62. Jeremias, G. *et al.* Transgenerational Inheritance of DNA Hypomethylation in *Daphnia magna* in Response to Salinity Stress. *Environ. Sci. Technol.* **52**, 10114–10123 (2018).

63. Asselman, J. *et al.* Bisulfite sequencing with daphnia highlights a role for epigenetics in regulating stress response to microcystis through preferential differential methylation of

serine and threonine amino acids. *Environ. Sci. Technol.* **51**, 924–931 (2017).

64. Trijau, M. *et al.* Transgenerational DNA Methylation Changes in *Daphnia magna* Exposed to Chronic γ Irradiation. *Environ. Sci. Technol.* **52**, 4331–4339 (2018).

65. Hearn, J., Pearson, M., Blaxter, M., Wilson, P. J. & Little, T. J. Genome-wide methylation is modified by caloric restriction in *Daphnia magna*. *BMC Genomics* **20**, 197 (2019).

66. Kluttgen, B., Dulmer, U., Engels, M. & Ratte, H. T. Adam , an Artificial Freshwater for the Culture of Zooplankton. *Water Resour.* **28**, 743–746 (1994).

67. Regier, J. C. *et al.* Arthropod relationships revealed by phylogenomic analysis of nuclear protein-coding sequences. *Nature* **463**, 1079–1083 (2010).

68. El-Gebali, S. *et al.* The Pfam protein families database in 2019. *Nucleic Acids Res.* **47**, D427–D432 (2019).

69. Papadopoulos, J. S. & Agarwala, R. COBALT: Constraint-based alignment tool for multiple protein sequences. *Bioinformatics* **23**, 1073–1079 (2007).

70. Aapola, U. *et al.* Isolation and Initial Characterization of a Novel Zinc Finger Gene , DNMT3L , on 21q22 . 3 , Related to the Cytosine-5- Methyltransferase 3 Gene Family. *Genomics* **65**, 293–298 (2000).

71. Gowher, H. *et al.* Mutational analysis of the catalytic domain of the murine Dnmt3a DNA-(cytosine C5)-methyltransferase. *J. Mol. Biol.* **357**, 928–941 (2006).

72. Mohamad Ishak, N. S., Kato, Y., Matsuura, T. & Watanabe, H. Sequence Conservation and Sexually Dimorphic Expression of the Ftz-F1 Gene in the Crustacean Daphnia magna. *PLoS One* **11**, e0154636 (2016).

73. Agatz, A., Hammers-Wirtz, M., Gergs, A., Mayer, T. & Preuss, T. G. Family-portraits for daphnids: scanning living individuals and populations to measure body length. *Ecotoxicology* **24**, 1385–1394 (2015).

74. Lampert, W. & Trubetskova, I. Juvenile Growth Rate as a Measure of Fitness in Daphnia. *Funct. Ecol.* **10**, 631 (1996).

75. Guibert, S. & Weber, M. *Functions of DNA Methylation and Hydroxymethylation in Mammalian Development*. *Current Topics in Developmental Biology* **104**, (2013).

76. Jain, D. *et al.* rahu is a mutant allele of Dnmt3c , encoding a DNA methyltransferase homolog required for meiosis and transposon repression in the mouse male germline. *PLoS Genet.* **13**, e1006964 (2017).

77. Barau, J. *et al.* The DNA methyltransferase DNMT3C protects male germ cells from transposon activity. *Science.* **354**, 909–912 (2016).

78. Wu, H. *et al.* Structural and histone binding ability characterizations of human PWWP domains. *PLoS One* **6**, (2011).

79. Qin, S. & Min, J. Structure and function of the nucleosome-binding PWWP domain. *Trends Biochem. Sci.* **39**, 536–547 (2014).

80. Chedin, F., Lieber, M. R. & Hsieh, C.-L. The DNA methyltransferase-like protein DNMT3L stimulates de novo methylation by Dnmt3a. *Proc. Natl. Acad. Sci. U. S. A.* **99**, 16916–21 (2002).

81. Eijkelenboom, A. & Burgering, B. M. T. FOXOs: Signalling integrators for homeostasis maintenance. *Nat. Rev. Mol. Cell Biol.* **14**, 83–97 (2013).

82. Koyama, T., Mendes, C. C. & Mirth, C. K. Mechanisms regulating nutrition-dependent developmental plasticity through organ-specific effects in insects. *Front. Physiol.* (2013).

83. Biggs, W. H., Cavenee, W. K. & Arden, K. C. Identification and characterization of members of the FKHR (FOX O) subclass of winged-helix transcription factors in the mouse. *Mamm. Genome* **12**, 416–425 (2001).

84. Zhang, W. *et al.* FoxO1 regulates multiple metabolic pathways in the liver effects on gluconeogenic, glycolytic, and lipogenic gene expression. *J. Biol. Chem.* **281**, 10105–10117 (2006).

85. Smith, Z. D. *et al.* A unique regulatory phase of DNA methylation in the early mammalian embryo. *Nature* **484**, 339–344 (2012).

86. Auclair, G., Guibert, S., Bender, A. & Weber, M. Ontogeny of CpG island methylation and specificity of DNMT3 methyltransferases during embryonic development in the mouse. *Genome Biol.* **15**, 1–16 (2014).

87. Kusari, F., O'Doherty, A. M., Hodges, N. J. & Wojewodzic, M. W. Bi-directional effects of vitamin B12 and methotrexate on Daphnia magna fitness and genomic methylation. *Sci. Rep.* **7**, 11872 (2017).

88. Okano, M., Bell, D. W., Haber, D. A. & Li, E. DNA Methyltransferases Dnmt3a and Dnmt3b Are Essential for De Novo Methylation and Mammalian Development. *Cell* **99**, 247–257 (1999).

89. de Mendoza, A. *et al.* Convergent evolution of a vertebrate-like methylome in a marine sponge. *Nat. Ecol. Evol.* **3**, 1464–1473 (2019).

90. Suzuki, M. M. & Bird, A. DNA methylation landscapes: provocative insights from epigenomics. *Nat. Rev. Genet.* **9**, 465–476 (2008).

91. Zemach, A., McDaniel, I. E., Silva, P. & Zilberman, D. Genome-Wide Evolutionary Analysis of Eukaryotic DNA Methylation. *Science.* **328**, 916 LP – 919 (2010).

92. Pegoraro, M., Bafna, A., Davies, N. J., Shuker, D. M. & Tauber, E. DNA methylation changes induced by long and short photoperiods in Nasonia. *Genome Res.* **26**, 203–210 (2016).

93. Li-byarlay, H. *et al.* RNA interference knockdown of DNA methyl- transferase 3 affects gene alternative splicing in the honey bee. *PNAS* **110**, 12750–12755 (2013).

94. Lindeman, L. C. *et al.* Epigenetic, transcriptional and phenotypic responses in two generations of Daphnia magna exposed to the DNA methylation inhibitor 5-azacytidine. *Environ. Epigenetics* **5**, 1–12 (2019).

95. Nguyen, N. D., Matsuura, T., Kato, Y. & Watanabe, H. Caloric restriction upregulates the expression of DNMT3.1, lacking the conserved catalytic domain, in Daphnia magna. *genesis* e23396 (2020). doi:https://doi.org/10.1002/dvg.23396

96. Honda, Y., Tsuchiya, K., Sumiyoshi, E., Haruta, N. & Sugimoto, A. Tubulin isotype substitution revealed that isotype combination modulates microtubule dynamics in C. elegans embryos. *J. Cell Sci.* **130**, 1652–1661 (2017).

97. Kato, Y. *et al.* Development of an RNA interference method in the cladoceran crustacean Daphnia magna. *Dev. Genes Evol.* **220**, 337–345 (2011).

98. Kato, Y. *et al.* Sequence divergence and expression of a transformer gene in the

branchiopod crustacean, Daphnia magna. *Genomics* **95**, 160–165 (2010).

99. Colbourne, J. K., Singan, V. R. & Gilbert, D. G. wFleaBase: The Daphnia genome database. *BMC Bioinformatics* **6**, 1–5 (2005).

100. Pijar, R. *et al.* Mutation of the cytochrome P450 CYP360A8 gene increased sensitivity to herbicide paraquat in Daphnia magna. *Environ. Toxicol. Chem.* (2020).

101. Ge, S. X., Son, E. W. & Yao, R. iDEP: An integrated web application for differential expression and pathway analysis of RNA-Seq data. *BMC Bioinformatics* **19**, 1–24 (2018).

102. Gura, M. A. *et al.* Dynamic and regulated TAF gene expression during mouse embryonic germ cell development. *PLoS Genet.* **16**, 1–28 (2020).

103. Conesa, A. & Götz, S. Blast2GO: A comprehensive suite for functional analysis in plant genomics. *Int. J. Plant Genomics* **2008**, (2008).

104. Colbourne, J. K. *et al.* Sampling Daphnia's expressed genes: Preservation, expansion and invention of crustacean genes with reference to insect genomes. *BMC Genomics* **8**, 1–19 (2007).

105. Jia, D., Jurkowska, R. Z., Zhang, X., Jeltsch, A. & Cheng, X. Structure of Dnmt3a bound to Dnmt3L suggests a model for de novo DNA methylation. *Nature* **449**, 248–51 (2007).

106. Liao, J. *et al.* Targeted disruption of DNMT1, DNMT3A and DNMT3B in human embryonic stem cells. *Nat. Genet.* **47**, 469–78 (2015).

107. Jiang, W., Bikard, D., Cox, D., Zhang, F. & Marraffini, L. A. RNA-guided editing of bacterial genomes using CRISPR-Cas systems. *Nat. Biotechnol.* **31**, 233–239 (2013).

108. Fu, Y. *et al.* High-frequency off-target mutagenesis induced by CRISPR-Cas nucleases in

human cells. *Nat. Biotechnol.* **31**, 822–826 (2013).

109. Rogina, B., Reenan, R. A., Nilsen, S. P. & Helfand, S. L. Extended Life-Span Conferred by Cotransporter Gene Mutations in Drosophila. *Science.* **290**, 2137–2140 (2000).

110. Wang, P.-Y. *et al.* Long-lived Indy and calorie restriction interact to extend life span. *Proc. Natl. Acad. Sci.* **106**, 9262–9267 (2009).

111. Rogers, R. P. & Rogina, B. The role of INDY in metabolism, health and longevity. *Front. Genet.* **6**, 204 (2015).

112. Nowialis, P. *et al.* Catalytically inactive Dnmt3b rescues mouse embryonic development by accessory and repressive functions. *Nat. Commun.* **10**, (2019).

113. Bownes, M. & Rembold, H. The titre of juvenile hormone during the pupal and adult stages of the life cycle of Drosophila melanogaster. *Eur. J. Biochem.* **164**, 709–712 (1987).

114. Broadus, J., McCabe, J. R., Endrizzi, B., Thummel, C. S. & Woodard, C. T. The Drosophila beta FTZ-F1 orphan nuclear receptor provides competence for stage-specific responses to the steroid hormone ecdysone. *Mol. Cell* **3**, 143–149 (1999).

115. Kato, Y., Tokishita, S. I., Ohta, T. & Yamagata, H. A vitellogenin chain containing a superoxide dismutase-like domain is the major component of yolk proteins in cladoceran crustacean Daphnia magna. *Gene* **334**, 157–165 (2004).

116. Tokishita, S. *et al.* Organization and repression by juvenile hormone of a vitellogenin gene cluster in the crustacean, Daphnia magna. *Biochem. Biophys. Res. Commun.* **345**, 362–370 (2006).

117. von Elert, E. *et al.* Protease activity in gut of Daphnia magna: evidence for trypsin and chymotrypsin enzymes. *Comp. Biochem. Physiol. Part B Biochem. Mol. Biol.* **137**, 287–296 (2004).

118. Harbison, S. T., Chang, S., Kamdar, K. P. & Mackay, T. F. C. Quantitative genomics of starvation stress resistance in Drosophila. *Genome Biol.* **6**, R36 (2005).

119. Cigolini, M. *et al.* Starvation-induced insulin resistance: Influence on 3-O-methylglucose transport. *Acta Diabetol. Lat.* **22**, 351–355 (1985).

120. Gross, D. N., van den Heuvel, A. P. J. & Birnbaum, M. J. The role of FoxO in the regulation of metabolism. *Oncogene* **27**, 2320–2336 (2008).